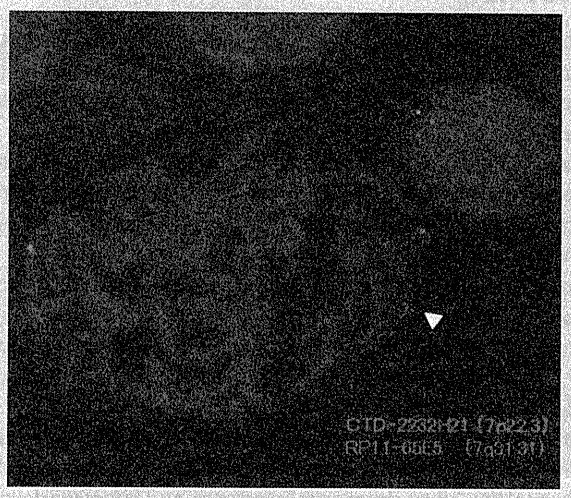

FIG. 3. FISH analyses of the patient. Arrow head indicates the deletion at 7q31.31.

[2010] characterized a de novo complex rearrangement of the long arm of chromosome 7 in a female patient with moderate mental retardation, anxiety disorder, and autistic features and suggested that disruption of the *C7orf58* gene contributed to the anxiety disorder, and autistic features of their patient. The *C7orf58* gene was also deleted in our patient. However, there have been no basic studies on the association of the *C7orf58* gene and brain function. Further studies are necessary on the role of the *C7orf58* gene.

Sadakata et al. [2007b] studied the behavior of *Cadps2−/−* mice. They showed impaired social interaction, hyperactivity, decreased exploratory behavior, and/or increased anxiety in a novel environment and deficits in intrinsic sleep–wake regulation and circadian rhythmicity. In addition, maternal neglect of newborns was a striking feature. They identified that *Cadps2−/−* mice show deficient release of NT-3 and BDNF. Cerebellar development was impaired in the mice. Sadakata et al. [2007a] found an aberrant alternatively spliced *CADPS2* mRNA that lacks exon 3 in some autistic patients. Exon 3 was shown to encode the dynactin 1-binding domain and affect axonal CADPS2 protein distribution. Exon 3-skipped CADPS2 protein possesses almost normal BDNF releasing activity but is not properly transported into the axons of neocortical or cerebellar neurons. However, Eran et al. [2009] observed no difference in prevalence of exon 3 skipping between ASDs and control samples. They concluded that exon 3 skipping represents a normal, minor isoform of CADPS2 in the cerebellum and is likely not a mechanism underlying autism susceptibility or pathogenesis. Our result may reinforce the evidence that *CADPS2* is associated with ASDs.

Cisternas et al. [2003] studied *CADPS2* gene mutations in 90 unrelated autistic individuals. However, they identified no disease-specific variants. Their results indicate that *CADPS2* mutations are not a major cause of ASDs. However, although small deletions of *CADPS2* as found in the present patient, might be rare, they support the idea that *CADPS2* abnormalities are associated with autism susceptibility.

Nikopoulos et al. [2010] reported two missense mutations in five of 11 FEVR families, indicating that mutations in *TSPAN12* are a relatively frequent cause of FEVR. Both residues are completely conserved throughout vertebrate evolution. These authors suggested that both haploinsufficiency and a dominant-negative effect of the mutant TSPAN12 on the wild-type protein should be considered as underlying disease mechanisms. Poulter et al. [2010] described mutations in the *TSPAN12* gene in FEVR patients and suggested that haploinsufficiency of *TSPAN12* causes FEVR because at least four of the seven mutations are predicted to lead to transcripts with premature-termination codons that are likely to be targeted by nonsense-mediated decay.

Recently, the Norrin/Frizzled4 signaling pathway that acts on the on the surface of developing endothelial cells and controls retinal vascular development is highlighted [Ye et al., 2010]. This pathway is composed of Norrin, its transmembrane receptor, Frizzled4, coreceptor, Lrp5, and an auxiliary membrane protein, Tspan12. The resulting signal controls a transcriptional program that regulates endothelial growth and maturation. PHPV and FEVR are associated with their pathogenesis. Our findings indicate that haploinsufficiency of *TSPAN12* is a plausible causative mechanism for PHPV. It will be interesting to study *TSPAN12* abnormalities in PHPV without *NDP* and *FZD4* mutations.

Singh et al. [2006] reported a voltage-gated potassium channel gene mutation in a temporal lobe epilepsy patient, namely a Kv4.2 truncation mutation lacking the last 44 amino acids in the carboxyl terminal. Kv4.2 channel is encoded by the *KCND2* gene. We suggest that the epileptic discharges on EEG reflect neuronal excitability caused by haploinsufficiency of *KCND2*.

Shen et al. [2010] suggested that using chromosomal microarray analysis to test for submicroscopic genomic deletions and duplications should be considered as part of the initial diagnostic evaluation of patients with ASDs. Miller et al. [2010] suggested that the use of chromosomal microarray is recommended as the first-tier cytogenetic diagnostic test for patients with unexplained developmental delay/intellectual disability, ASDs, or multiple congenital anomalies. In patients with ASDs and other anomalies, chromosomal microarray may be the useful method to clarify the underlying defect.

ACKNOWLEDGMENTS

We thank the patient's family for their cooperation. This study was supported by Health and Labour Research Grants from the Ministry of Health, Labour and Welfare of Japan.

REFERENCES

Alarcón M, Abrahams BS, Stone JL, Duvall JA, Perederiy JV, Bomar JM, Sebat J, Wigler M, Martin CL, Ledbetter DH, Nelson SF, Cantor RM, Geschwind DH. 2008. Linkage, association, and gene-expression analyses identify CNTNAP2 as an autism-susceptibility gene. Am J Hum Genet 82:150–159.

Arking DE, Cutler DJ, Brune CW, Teslovich TM, West K, Ikeda M, Rea A, Guy M, Lin S, Cook EH, Chakravarti A. 2008. A common genetic variant in the neurexin superfamily member CNTNAP2 increases familial risk of autism. Am J Hum Genet 82:160–164.

Berkel S, Marshall CR, Weiss B, Howe J, Roeth R, Moog U, Endris V, Roberts W, Szatmari P, Pinto D, Bonin M, Riess A, Engels H, Sprengel R, Scherer SW, Rappold GA. 2010. Mutations in the SHANK2 synaptic scaffolding gene in autism spectrum disorder and mental retardation. Nat Genet 42:489–491.

Bonora E, Lamb JA, Barnby G, Sykes N, Moberly T, Beyer KS, Klauck SM, Poustka F, Bacchelli E, Blasi F, Maestrini E, Battaglia A, Haracopos D, Pedersen L, Isager T, Eriksen G, Viskum B, Sorensen EU, Brondum-Nielsen K, Cotterill R, Engeland H, Jonge M, Kemner C, Steggehuis K, Scherpenisse M, Rutter M, Bolton PF, Parr JR, Poustka A, Bailey AJ, Monaco AP, International Molecular Genetic Study of Austism Consortium. 2005. Mutation screening and association analysis of six candidate genes for autism on chromosome 7q. Eur J Hum Genet 13:198–207.

Cisternas FA, Vincent JB, Scherer SW, Ray PN. 2003. Cloning and characterization of human CADPS and CADPS2, new members of the Ca^{2+}-dependent activator for secretion protein family. Genomics 81: 279–291.

Cukier HN, Skaar DA, Rayner-Evans MY, Konidari I, Whitehead PL, Jaworski JM, Cuccaro ML, Pericak-Vance MA, Gilbert JR. 2009. Identification of chromosome 7 inversion breakpoints in an autistic family narrows candidate region for autism susceptibility. Autism Res 2: 258–266.

Dauwerse JG, Ruivenkamp CA, Hansson K, Marijnissen GM, Peters DJ, Breuning MH, Hilhorst-Hofstee Y. 2010. A complex chromosome 7q rearrangement identified in a patient with mental retardation, anxiety disorder, and autistic features. Am J Med Genet Part A 152A:427–433.

Durand CM, Betancur C, Boeckers TM, Bockmann J, Chaste P, Fauchereau F, Nygren G, Rastam M, Gillberg IC, Anckarsäter H, Sponheim E, Goubran-Botros H, Delorme R, Chabane N, Mouren-Simeoni MC, de Mas P, Bieth E, Rogé B, Héron D, Burglen L, Gillberg C, Leboyer M, Bourgeron T. 2007. Mutations in the gene encoding the synaptic scaffolding protein SHANK3 are associated with autism spectrum disorders. Nat Genet 39:25–27.

Eran A, Graham KR, Vatalaro K, McCarthy J, Collins C, Peters H, Brewster SJ, Hanson E, Hundley R, Rappaport L, Holm IA, Kohane IS, Kunkel LM. 2009. Comment on "Autistic-like phenotypes in Cadps2-knockout mice and aberrant CADPS2 splicing in autistic patients". J Clin Invest 119: 679–680.

Glessner JT, Wang K, Cai G, Korvatska O, Kim CE, Wood S, Zhang H, Estes A, Brune CW, Bradfield JP, Imielinski M, Frackelton EC, Reichert J, Crawford EL, Munson J, Sleiman PM, Chiavacci R, Annaiah K, Thomas K, Hou C, Glaberson W, Flory J, Otieno F, Garris M, Soorya L, Klei L, Piven J, Meyer KJ, Anagnostou E, Sakurai T, Game RM, Rudd DS, Zurawiecki D, McDougle CJ, Davis LK, Miller J, Posey DJ, Michaels S, Kolevzon A, Silverman JM, Bernier R, Levy SE, Schultz RT, Dawson G, Owley T, McMahon WM, Wassink TH, Sweeney JA, Nurnberger JI, Coon H, Sutcliffe JS, Minshew NJ, Grant SF, Bucan M, Cook EH, Buxbaum JD, Devlin B, Schellenberg GD, Hakonarson H. 2009. Autism genome-wide copy number variation reveals ubiquitin and neuronal genes. Nature 459:569–573.

International Molecular Genetic Study of Autism Consortium. 1998. A full genome screen for autism with evidence for linkage to a region on chromosome 7q. Hum Mol Genet 7:571–578.

International Molecular Genetic Study of Autism Consortium (IMGSAC). 2001. Further characterization of the autism susceptibility locus AUTS1 on chromosome 7q. Hum Mol Genet 10:973–982.

Jamain S, Quach H, Betancur C, Råstam M, Colineaux C, Gillberg IC, Soderstrom H, Giros B, Leboyer M, Gillberg C, Bourgeron T. Paris Autism Research International Sibpair Study. 2003. Mutations of the X-linked genes encoding neuroligins NLGN3 and NLGN4 are associated with autism. Nat Genet 34:27–29.

Junge HJ, Yang S, Burton JB, Paes K, Shu X, French DM, Costa M, Rice DS, Ye W. 2009. TSPAN12 regulates retinal vascular development by promoting Norrin- but not Wnt-induced FZD4/beta-catenin signaling. Cell 139:299–311.

Kim HG, Kishikawa S, Higgins AW, Seong IS, Donovan DJ, Shen Y, Lally E, Weiss LA, Najm J, Kutsche K, Descartes M, Holt L, Braddock S, Troxell R, Kaplan L, Volkmar F, Klin A, Tsatsanis K, Harris DJ, Noens I, Pauls DL, Daly MJ, MacDonald ME, Morton CC, Quade BJ, Gusella JF. 2008. Disruption of neurexin 1 associated with autism spectrum disorder. Am J Hum Genet 82:199–207.

Lennon PA, Cooper ML, Peiffer DA, Gunderson KL, Patel A, Peters S, Cheung SW, Bacino CA. 2007. Deletion of 7q31.1 supports involvement of FOXP2 in language impairment: Clinical report and review. Am J Med Genet A 143A:791–798.

Marshall CR, Noor A, Vincent JB, Lionel AC, Feuk L, Skaug J, Shago M, Moessner R, Pinto D, Ren Y, Thiruvahindrapduram B, Fiebig A, Schreiber S, Friedman J, Ketelaars CE, Vos YJ, Ficicioglu C, Kirkpatrick S, Nicolson R, Sloman L, Summers A, Gibbons CA, Teebi A, Chitayat D, Weksberg R, Thompson A, Vardy C, Crosbie V, Luscombe S, Baatjes R, Zwaigenbaum L, Roberts W, Fernandez B, Szatmari P, Scherer SW. 2008. Structural variation of chromosomes in autism spectrum disorder. Am J Hum Genet 82:477–488.

Miller DT, Adam MP, Aradhya S, Biesecker LG, Brothman AR, Carter NP, Church DM, Crolla JA, Eichler EE, Epstein CJ, Faucett WA, Feuk L, Friedman JM, Hamosh A, Jackson L, Kaminsky EB, Kok K, Krantz ID, Kuhn RM, Lee C, Ostell JM, Rosenberg C, Scherer SW, Spinner NB, Stavropoulos DJ, Tepperberg JH, Thorland EC, Vermeesch JR, Waggoner DJ, Watson MS, Martin CL, Ledbetter DH. 2010. Consensus statement: Chromosomal microarray is a first-tier clinical diagnostic test for individuals with developmental disabilities or congenital anomalies. Am J Hum Genet 86:749–764.

Moessner R, Marshall CR, Sutcliffe JS, Skaug J, Pinto D, Vincent J, Zwaigenbaum L, Fernandez B, Roberts W, Szatmari P, Scherer SW. 2007. Contribution of SHANK3 mutations to autism spectrum disorder. Am J Hum Genet 81:1289–1297.

Nikopoulos K, Gilissen C, Hoischen A, van Nouhuys CE, Boonstra FN, Blokland EA, Arts P, Wieskamp N, Strom TM, Ayuso C, Tilanus MA, Bouwhuis S, Mukhopadhyay A, Scheffer H, Hoefsloot LH, Veltman JA, Cremers FP, Collin RW. 2010. Next-generation sequencing of a 40 Mb linkage interval reveals TSPAN12 mutations in patients with familial exudative vitreoretinopathy. Am J Hum Genet 86:240–247.

Poulter JA, Ali M, Gilmour DF, Rice A, Kondo H, Hayashi K, Mackey DA, Kearns LS, Ruddle JB, Craig JE, Pierce EA, Downey LM, Mohamed MD, Markham AF, Inglehearn CF, Toomes C. 2010. Mutations in TSPAN12 cause autosomal-dominant familial exudative vitreoretinopathy. Am J Hum Genet 86:248–253.

Sadakata T, Washida M, Iwayama Y, Shoji S, Sato Y, Ohkura T, Katoh-Semba R, Nakajima M, Sekine Y, Tanaka M, Nakamura K, Iwata Y, Tsuchiya KJ, Mori N, Detera-Wadleigh SD, Ichikawa H, Itohara S, Yoshikawa T, Furuichi T. 2007a. Autistic-like phenotypes in Cadps2-knockout mice and aberrant CADPS2 splicing in autistic patients. J Clin Invest 117:931–943.

Sadakata T, Kakegawa W, Mizoguchi A, Washida M, Katoh-Semba R, Shutoh F, Okamoto T, Nakashima H, Kimura K, Tanaka M, Sekine Y, Itohara S, Yuzaki M, Nagao S, Furuichi T. 2007b. Impaired cerebellar development and function in mice lacking CAPS2, a protein involved in neurotrophin release. J Neurosci 27:2472–2482.

Sadakata T, Washida M, Furuichi T. 2007c. Alternative splicing variations in mouse CAP S2: Differential expression and functional properties of splicing variants. BMC Neurosci 8:25.

Sebat J, Lakshmi B, Malhotra D, Troge J, Lese-Martin C, Walsh T, Yamrom B, Yoon S, Krasnitz A, Kendall J, Leotta A, Pai D, Zhang R, Lee YH, Hicks

J, Spence SJ, Lee AT, Puura K, Lehtimäki T, Ledbetter D, Gregersen PK, Bregman J, Sutcliffe JS, Jobanputra V, Chung W, Warburton D, King MC, Skuse D, Geschwind DH, Gilliam TC, Ye K, Wigler M. 2007. Strong association of de novo copy number mutations with autism. Science 316:445–449.

Shastry BS. 2009. Persistent hyperplastic primary vitreous: Congenital malformation of the eye. Clin Experiment Ophthalmol 37:884–890.

Shen Y, Dies KA, Holm IA, Bridgemohan C, Sobeih MM, Caronna EB, Miller KJ, Frazier JA, Silverstein I, Picker J, Weissman L, Raffalli P, Jeste S, Demmer LA, Peters HK, Brewster SJ, Kowalczyk SJ, Rosen-Sheidley B, McGowan C, Duda AW III, Lincoln SA, Lowe KR, Schonwald A, Robbins M, Hisama F, Wolff R, Becker R, Nasir R, Urion DK, Milunsky JM, Rappaport L, Gusella JF, Walsh CA, Wu BL, Miller DT. Autism Consortium Clinical Genetics/DNA Diagnostics Collaboration. 2010. Clinical genetic testing for patients with autism spectrum disorders. Pediatrics 125:e727–e735.

Shimojima K, Páez MT, Kurosawa K, Yamamoto T. 2009. Proximal interstitial 1p36 deletion syndrome: The most proximal 3.5-Mb microdeletion identified on a dysmorphic and mentally retarded patient with inv(3)(p14.1q26.2). Brain Development 31:629–633.

Singh B, Ogiwara I, Kaneda M, Tokonami N, Mazaki E, Baba K, Matsuda K, Inoue Y, Yamakawa K. 2006. A Kv4.2 truncation mutation in a patient with temporal lobe epilepsy. Neurobiol Dis 24:245–253.

Ye X, Wang Y, Nathans J. 2010. The Norrin/Frizzled4 signaling pathway in retinal vascular development and disease. Trends Mol Med 16:417–425.

RESEARCH ARTICLE

AMERICAN JOURNAL OF medical genetics PART A

Submicroscopic Deletion of 12q13 Including *HOXC* Gene Cluster With Skeletal Anomalies and Global Developmental Delay

Nobuhiko Okamoto,[1]* Daisuke Tamura,[2] Gen Nishimura,[3] Keiko Shimojima,[4] and Toshiyuki Yamamoto[4]

[1]Department of Medical Genetics, Osaka Medical Center and Research Institute for Maternal and Child Health, Osaka, Japan

[2]Department of Orthopedics, Osaka Medical Center and Research Institute for Maternal and Child Health, Osaka, Japan

[3]Department of Pediatric Imaging, Tokyo Metropolitan Children's Medical Center, Tokyo, Japan

[4]Tokyo Women's Medical University Institute for Integrated Medical Sciences, Tokyo, Japan

Received 13 May 2011; Accepted 4 September 2011

We report on a patient with a submicroscopic deletion of 12q13 detected by array-CGH and confirmed by FISH. He was haploinsufficient for the *HOXC* gene cluster and some other neighboring genes. *HOX* genes have an important role in the initial formation of the body. The patient showed characteristic features including severe kyphoscoliosis, digital abnormalities, cardiac anomaly, expressive language, and global developmental delay. Radiologic features of the fingers had some similarities with those for multiple synostosis syndrome. No human genetic disorders due to *HOXC* abnormalities are yet known. We tentatively assume that his skeletal anomalies are associated with haploinsufficiency of the *HOXC* gene cluster. Further studies are necessary to determine the clinical importance of haploinsufficiency of the *HOXC* gene cluster.

Key words: *HOX*; *HOXC*; array-CGH; kyphoscoliosis; multiple synostosis syndrome

How to Cite this Article:
Okamoto N, Tamura D, Nishimura G, Shimojima K, Yamamoto T. 2011. Submicroscopic deletion of 12q13 including *HOXC* gene cluster with skeletal anomalies and global developmental delay.
Am J Med Genet Part A 155:2997–3001.

INTRODUCTION

HOX genes have an important role in the initial formation of the body plan by providing positional information along the anterior–posterior body and limb axis and are associated with neural tube closure. *HOX* A, B, C, and D make a cluster on chromosomes 7, 17, 12, and 2, respectively. Each cluster consists of 9–11 genes from 13 paralogous groups. The order of the *HOX* genes along the chromosome correlates with their expression along the anterior/posterior axis of the embryo.

Some of the *HOX* genes are associated with genetic syndromes. Akarsu et al. [1996] reported that a polyalanine tract expansion in *HOXD13* causes synpolydactyly (OMIM #186000). Mortlock and Innis [1997] found a nonsense mutation in *HOXA13* among patients with hand-foot-genital syndrome (OMIM #140000). Thompson and Nguyen [2000] reported that megakaryocytic thrombocytopenia and radio-ulnar synostosis (OMIM #605432) are associated with *HOXA11* mutations. Shrimpton et al. [2004] reported a *HOXD10* mutation in a family with isolated congenital vertical talus and Charcot-Marie-Tooth disease (OMIM #142984). Tischfield et al. [2005] identified homozygous truncating mutations in *HOXA1* in patients with horizontal gaze abnormalities, deafness, facial weakness, hypoventilation, vascular malformations of the internal carotid arteries and cardiac outflow tract, intellectual disability, and autism spectrum disorder. Two syndromes associated with homozygous mutations of *HOXA1* are known as the Bosley-Salih-Alorainy syndrome and the Athabascan brainstem dysgenesis syndrome (OMIM #601536) [Bosley et al., 2008]. Alasti et al. [2008] reported a mutation in *HOXA2* in autosomal-recessive microtia (OMIM #612290).

Spitz et al. [2002] reported a t(2;8)(q31;p21) balanced translocation with breakpoints near the human *HOXD* complex. The patient had mesomelic dysplasia of the upper limbs and vertebral defects. Dlugaszewska et al. [2006] reported three patients with limb abnormalities and breakpoints involving chromosome 2q31. None of the three 2q31 breakpoints, which all mapped close to the *HOXD*

Additional supporting information may be found in the online version of this article.

Grant sponsor: Ministry of Health, Labour, and Welfare in Japan.

*Correspondence to:
Dr. Nobuhiko Okamoto, Department of Medical Genetics, Osaka Medical Center and Research Institute for Maternal and Child Health, 840 Murodo-cho, Izumi, Osaka 594-1101, Japan. E-mail: okamoto@osaka.email.ne.jp

Published online 8 November 2011 in Wiley Online Library (wileyonlinelibrary.com).
DOI 10.1002/ajmg.a.34324

cluster, disrupted any known genes. They suggested that the three rearrangements disturb normal *HOXD* gene regulation by position effects. Yue et al. [2007] reported a boy with severe intellectual disability, funnel chest, bell-shaped thorax, and hexadactyly of both feet. The patient had a balanced de novo t(12;17)(p13.3;q21.3) translocation. The breakpoint was near the *HOXB* cluster. They proposed that misregulation of a *HOXB* gene(s) by position effect is responsible for the patient's phenotype. Jun et al. [2011] reported a patient with the *HOXA* cluster deletion with manifestations similar to those observed in hand-foot-genital syndrome, which is caused by a haploinsufficiency of *HOXA13*.

We report on a patient with distinctive skeletal anomalies with a submicroscopic deletion of 12q13. He was haploinsufficient for the *HOXC* gene cluster. So far, no human genetic disorders due to *HOXC* abnormalities are reported. We discuss the clinical features in the patient and the haploinsufficiency of the *HOXC* genes.

CLINICAL REPORT

The 14-year-old male propositus was the first-born child of a 26-year-old mother and a 30-year-old father, both healthy and non-consanguineous. After an uncomplicated pregnancy, he was born at 39 weeks of gestation by induced delivery. His length was 53 cm (90th centile). His birth weight was 3,010 g, within normal limits (25th centile). After birth, cardiac murmur was noticed. Echocardiography revealed tetralogy of Fallot. Cardiac surgery was carried out successfully at 2 years of age. Surgery for bilateral inguinal hernia and strabismus was done at 3 years of age. His dentition was abnormal. Persistent teeth erupted before the loss of primary teeth. He showed hypodontia.

His development was delayed since early infancy. From the age of 6 months, he received physical training for delayed motor development. He was able to roll over at 10 months of age, and to sit alone at 3 years of age. He started to walk independently at 5 years of age and the spine deformity appeared. His global development quotient was 20 at 3 years of age. He attended special education in school. Gradually, he could understand simple words. His intellectual quotient remained around 30 and verbal production was almost absent. However, recently he could express simple sentences using key boards.

Physical examination identified dysmorphic features, including a long face, a broad nose, prominent ears, bilateral low-set ears, downslanting palpebral fissures and a high palate. Severe kyphosis and mild scoliosis were remarkable features. The radial heads were dislocated bilaterally. Camptodactyly of middle and ring fingers, inflexible distal interphalangeal joints of index fingers and adducted thumbs of both hands were noted (Fig. 1A). Hearing and visual acuity were normal. His weight was 29 kg (<3rd centile), and his length was 160 cm (<3rd centile). His head circumference was average for his age, 14 years.

Radiographic analysis revealed severe kyphosis and mild scoliosis in the thoracic spine (Fig. 2A,B). The upper thorax was mildly narrowed. The proximal interphalangeal joints of both the middle and ring fingers showed flexion contracture with para-articular swelling (Fig. 1B). The proximal interphalangeal joints of both index fingers were swollen as well. The metacarpophalangeal joint of the right index finger and proximal interphalangeal joint of the left little finger showed ulnar deviation. The metacarpals were mildly undertubulated. Radiologic features of the fingers were like those seen in multiple synostosis syndrome. However, no carpal or tarsal coalition was found.

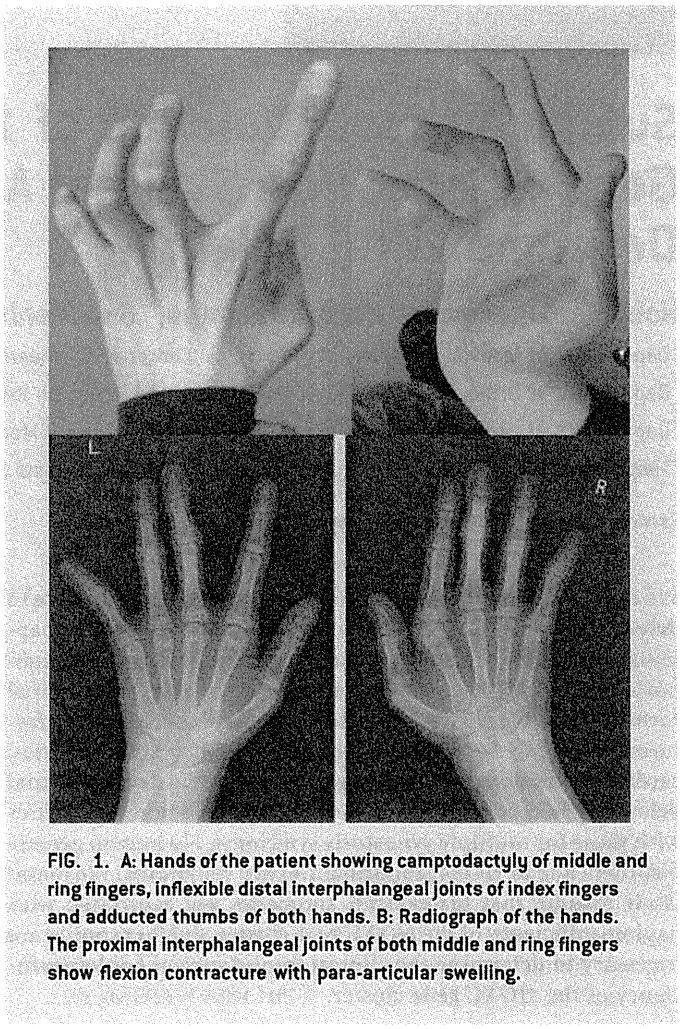

FIG. 1. A: Hands of the patient showing camptodactyly of middle and ring fingers, inflexible distal interphalangeal joints of index fingers and adducted thumbs of both hands. B: Radiograph of the hands. The proximal interphalangeal joints of both middle and ring fingers show flexion contracture with para-articular swelling.

Results of neuroradiological examinations including brain CT and MRI were normal. Routine laboratory tests were normal. His karyotype by G-banded analysis was 46,XY. Array-CGH analyses were performed to look for submicroscopic chromosomal aberrations.

MATERIALS AND METHODS

After obtaining informed consent and the permission of the institution's ethics committee, peripheral blood samples were drawn from the patient and his parents. Genomic DNA was extracted using the QIAquick DNA extraction kit (Qiagen, Valencia, CA).

Based on the hypothesis that the patient might have submicroscopic chromosomal aberrations, array-CGH analysis was performed using the Human Genome CGH Microarray 60K (Agilent Technologies, Santa Clara, CA) as described previously [Shimojima et al., 2009].

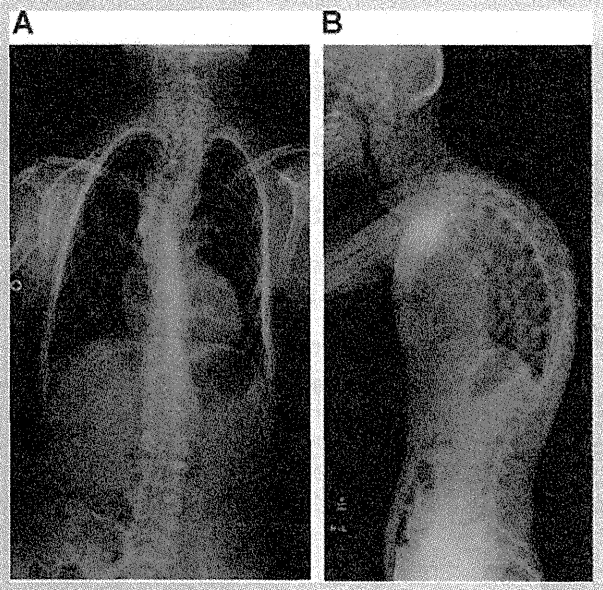

FIG. 2. Radiographs of the spine. A: Frontal view showing severe kyphosis and mild scoliosis in the thoracic spine. The upper thorax is mildly narrow. B: Lateral view.

Metaphase nuclei were prepared from peripheral blood lymphocytes by standard methods and used for FISH with human BAC clones selected from the UCSC genome browser (http://www.genome.ucsc.edu) as described elsewhere [Shimojima et al., 2009]. Physical positions refer to the March 2006 human reference sequence (NCBI Build 36.1).

RESULTS

By array-CGH analysis, loss of genomic copy numbers was identified in the region 12q13, which included the *HOXC* cluster (Fig. 3). The size of the deletion was 1.7 Mb. FISH analyses confirmed the deletion (see Supplementary Fig. A). FISH analyses of the parents found the deletion was de novo (data not shown). The karyotype of the patient was arr 12q13.1 (51,965,307-53,642,659)×1 dn.

DISCUSSION

A patient with distinctive skeletal anomalies had a submicroscopic deletion of 12q13 including *HOXC* gene cluster. His features included tetralogy of Fallot, abnormal dentition, and global developmental delay. This is the first report of *HOXC* gene cluster deletion. Human genetic disorders due to *HOXC* abnormalities are not known.

There have been multiple knock out studies on *Hoxc* genes. *Hoxc-4* is expressed in the most anterior regions of the CNS and prevertebral column. *Hoxc-4* mutant (−/−) mice showed a partial posterior homeotic transformation of the 7th cervical vertebra [Saegusa et al., 1996]. In addition, anterior transformations of the 3rd and 8th thoracic vertebrae, and an aperture or a fissure in the xiphoid process of the sternum were observed. No obvious defects were observed in the CNS. *Hoxc-4* (−/−) mice manifested vertebral defects that extended from the 2nd to 11th thoracic vertebra and died because of esophageal stenosis [Boulet and Capecchi, 1996].

Hoxc-8 is expressed in the limbs, backbone rudiments, and neural tube of mouse midgestation embryos, and in the cartilage and skeleton of newborns. Le Mouellic et al. [1992] generated *Hoxc-8* (−/−) mice. The mice were born alive, but most of them died within a few days. Anterior transformation in the several skeletal segments was characteristic. The 8th pair of ribs attached to the sternum and the 14th pair of ribs appeared on the 1st lumbar vertebra. During embryogenesis, *Hoxc-8* is highly expressed in motoneurons within spinal cord segments C7 to T1. These motoneurons innervate forelimb distal muscles that move the forepaw. *Hoxc-8*-deficient mice showed a congenital prehension deficiency of the forepaw due to abnormal innervation [Tiret et al., 1998].

Suemori et al. [1995] generated *Hoxc-9* mutant mice. Homozygous mice showed an anterior homeotic transformation from the 10th thoracic vertebra to the first lumbar vertebra. Bending and fusion of the ribs were observed. Eight or nine pairs of ribs were attached to the sternum. The sternum showed an abnormal pattern of ossification. Phenotypes of the mutant mice resembled those of the *Hoxc-8* mutant mice. Functional interaction between *Hoxc-8* and *Hoxc-9* during segmental determination was suspected.

Godwin and Capecchi [1998] reported *Hoxc-13* expression in the nails, tail, vibrissae, and filiform papillae of the tongue, and in hair follicles throughout the body. Mice homozygous for mutant alleles of *Hoxc-13* show brittle hair resulting in alopecia.

Suemori and Noguchi [2000] produced *Hox C* cluster null (−/−) mice. These mice die soon after birth with minor transformations. Perinatal death of the *HoxC* cluster (−/−) mutant mice is thought to be attributable to a neuromuscular defect in respiratory organs. Gross appearance of the skeleton and internal organs was almost normal. The mutant mouse showed subtle vertebral and rib anomalies. Malformations in the skeleton were even milder than those observed in some single gene mutant mice of *HoxC* genes. This means that at least some genes within a cluster interact with each other. The phenotype of *HoxC* cluster (+/−) mice, which have a similar genetic condition to our patient, was normal.

The phenotype of knockout mice does not always correspond to human disorders. Skeletal manifestations in our patient were not evident in his early childhood. Skeletal changes may progress during growth. Interestingly, translocation breakpoint near *HOXB* and *HOXD* with positional effect caused thoracic deformities and digital abnormalities [Spitz et al., 2002; Dlugaszewska et al., 2006; Yue et al., 2007]. We tentatively assume that skeletal anomalies in our patient are associated with haploinsufficiency of the *HOXC* gene cluster.

Radiologic features of the fingers had some similarities with those for multiple synostosis syndrome (OMIM #186500). Shi et al. [1999] found that Smad1 dislodges Hoxc-8 from its DNA-binding element and result in the induction of gene expression. Bone morphogenetic proteins (BMPs) induce osteoblast differentiation and bone formation. Smad1 mediates signaling initiated by BMPs and activates osteopontin and osteoprotegerin gene expression by dislodging Hoxc-8 from its DNA-binding sites [Liu et al., 2004].

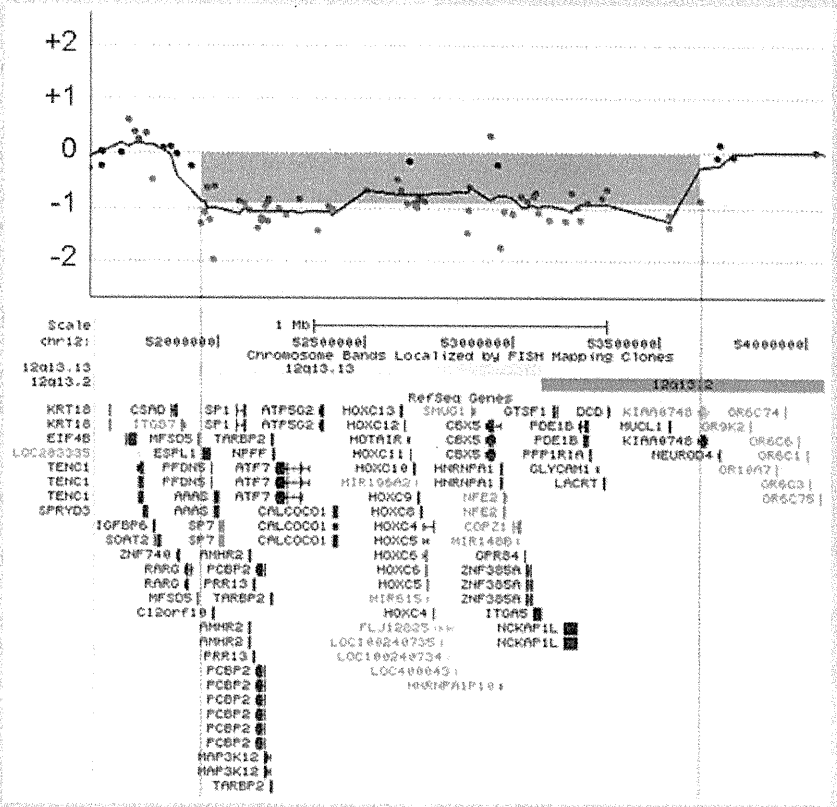

FIG. 3. Array-CGH revealed a loss of genomic copy numbers in the region 12q13, which included the *HOXC* cluster.

These findings indicate that *HOXC8* deficiency may induce osteogenesis by activating osteopontin and osteoprotegerin. The manifestations similar to the multiple synostosis syndrome, the flexion contracture and other digital abnormalities in our patient, may have some association with the *HOXC8* haploinsufficiency.

The multiple genes involved in the deletion may contribute to the manifestations. Our patient was haploinsuffient for *SP7/OSX*, *AAAS*, and *AMHRII*. Lapunzina et al. [2010] reported a homozygous single base pair deletion (c.1052delA) in *SP7/OSX* in an Egyptian child with recessive osteogenesis imperfecta (OMIM #613849). *SP7/OSX* plays a key role in human bone development. The triple-A syndrome (OMIM #231550) is caused by mutation in the gene-encoding aladin (*AAAS*; OMIM 605378). The anti-Müllerian hormone type II (AMHRII) receptor is the primary receptor for anti-Müllerian hormone (AMH), a protein responsible for the regression of the Müllerian duct in males. Mutations in the *AMHRII* gene lead to persistent Müllerian duct syndrome (OMIM #261550) in human males [Belville et al., 2009]. These syndromes are transmitted in autosomal recessive fashion and are not responsible for the manifestations in our patient. A haploinsufficiency of other genes may contribute to cardiac anomalies, dental anomalies, and intellectual disability with severe expressive language delay. Some of the deleted genes including *GPR84*, *PDE1B*, and *NPFF* are expressed in the nervous system. However, contribution of these genes to language development is unclear.

In conclusion, we report on a patient with distinctive skeletal anomalies and intellectual disability with a submicroscopic deletion of 12q13 including *HOXC* gene cluster. No human genetic disorders due to *HOXC* abnormalities are yet known. We posit that his kyphoscoliosis and digital abnormalities may be associated with haploinsufficiency of the *HOXC* gene cluster. Further studies of patients with similar conditions are necessary to determine the clinical significance of haploinsufficiency of the *HOXC* gene cluster.

ACKNOWLEDGMENTS

We thank for the family for their cooperation. This study was supported by the Health and Labour Research Grants in 2010 by Ministry of Health, Labour and Welfare in Japan.

REFERENCES

Akarsu AN, Stoilov I, Yilmaz E, Sayli BS, Sarfarazi M. 1996. Genomic structure of HOXD13 gene: A nine polyalanine duplication causes synpolydactyly in two unrelated families. Hum Mol Genet 5:945–952.

Alasti F, Sadeghi A, Sanati MH, Farhadi M, Stollar E, Somers T, Van Camp G. 2008. A mutation in HOXA2 is responsible for autosomal-recessive microtia in an Iranian family. Am J Hum Genet 82:982–991.

Belville C, Maréchal JD, Pennetier S, Carmillo P, Masgrau L, Messika-Zeitoun L, Galey J, Machado G, Treton D, Gonzalès J, Picard JY, Josso N, Cate RL, di Clemente N. 2009. Natural mutations of the anti-Mullerian hormone type II receptor found in persistent Mullerian duct syndrome affect ligand binding, signal transduction and cellular transport. Hum Mol Genet 18:3002–3013.

Bosley TM, Alorainy IA, Salih MA, Aldhalaan HM, Abu-Amero KK, Oystreck DT, Tischfield MA, Engle EC, Erickson RP. 2008. The clinical spectrum of homozygous HOXA1 mutations. Am J Med Genet A 146A:1235–1240.

Boulet AM, Capecchi MR. 1996. Targeted disruption of hoxc-4 causes esophageal defects and vertebral transformations. Dev Biol 177:232–249.

Dlugaszewska B, Silahtaroglu A, Menzel C, Kübart S, Cohen M, Mundlos S, Tümer Z, Kjaer K, Friedrich U, Ropers HH, Tommerup N, Neitzel H, Kalscheuer VM. 2006. Breakpoints around the HOXD cluster result in various limb malformations. J Med Genet 43:111–118.

Godwin AR, Capecchi MR. 1998. Hoxc13 mutant mice lack external hair. Genes and Dev 12:11–20.

Jun KR, Seo EJ, Lee JO, Yoo HW, Park IS, Yoon HK. 2011. Molecular cytogenetic and clinical characterization of a patient with a 5.6-Mb deletion in 7p15 including HOXA cluster. Am J Med Genet Part A 155A:642–647.

Lapunzina P, Aglan M, Temtamy S, Caparrós-Martín JA, Valencia M, Letón R, Martínez-Glez V, Elhossini R, Amr K, Vilaboa N, Ruiz-Perez VL. 2010. Identification of a frameshift mutation in Osterix in a patient with recessive osteogenesis imperfecta. Am J Hum Genet 87:110–114.

Le Mouellic H, Lallemand Y, Brûlet P. 1992. Homeosis in the mouse induced by a null mutation in the Hox-3.1 gene. Cell 69:251–264.

Liu Z, Shi W, Ji X, Sun C, Jee WS, Wu Y, Mao Z, Nagy TR, Li Q, Cao X. 2004. Molecules mimicking Smad1 interacting with Hox stimulate bone formation. J Biol Chem 279:11313–11319.

Mortlock DP, Innis JW. 1997. Mutation of HOXA13 in hand-foot-genital syndrome. Nat Genet 15:179–180.

Saegusa H, Takahashi N, Noguchi S, Suemori H. 1996. Targeted disruption in the mouse Hoxc-4 locus results in axial skeleton homeosis and malformation of the xiphoid process. Dev Biol 174:55–64.

Shi X, Yang X, Chen D, Chang Z, Cao X. 1999. Smad1 interacts with homeobox DNA-binding proteins in bone morphogenetic protein signaling. J Biol Chem 274:13711–13717.

Shimojima K, Páez MT, Kurosawa K, Yamamoto T. 2009. Proximal interstitial 1p36 deletion syndrome: The most proximal 3.5-Mb microdeletion identified on a dysmorphic and mentally retarded patient with inv(3)(p14.1q26.2). Brain and Development 31:629–633.

Shrimpton AE, Levinsohn EM, Yozawitz JM, Packard DS Jr, Cady RB, Middleton FA, Persico AM, Hootnick DR. 2004. A HOX gene mutation in a family with isolated congenital vertical talus and Charcot-Marie-Tooth disease. Am J Hum Genet 75:92–96.

Spitz F, Montavon T, Monso-Hinard C, Morris M, Ventruto ML, Antonarakis S, Ventruto V, Duboule D. 2002. A t(2;8) balanced translocation with breakpoints near the human HOXD complex causes mesomelic dysplasia and vertebral defects. Genomics 79:493–498.

Suemori H, Noguchi S. 2000. Hox C cluster genes are dispensable for overall body plan of mouse embryonic development. Dev Biol 220:333–342.

Suemori H, Takahashi N, Noguchi S. 1995. Hoxc-9 mutant mice show anterior transformation of the vertebrae and malformation of the sternum and ribs. Mech Dev 51:265–273.

Thompson AA, Nguyen LT. 2000. Amegakaryocytic thrombocytopenia and radio-ulnar synostosis are associated with HOXA11 mutation. Nat Genet 26:397–398.

Tiret L, Le Mouellic H, Maury M, Bru?let P. 1998. Increased apoptosis of motoneurons and altered somatotopic maps in the brachial spinal cord of Hoxc-8-deficient mice. Development 125:279–291.

Tischfield MA, Bosley TM, Salih MA, Alorainy IA, Sener EC, Nester MJ, Oystreck DT, Chan WM, Andrews C, Erickson RP, Engle EC. 2005. Homozygous HOXA1 mutations disrupt human brainstem, inner ear, cardiovascular and cognitive development. Nat Genet 37:1035–1037.

Yue Y, Farcas R, Thiel G, Bommer C, Grossmann B, Galetzka D, Kelbova C, Küpferling P, Daser A, Zechner U, Haaf T. 2007. De novo t(12;17)(p13.3;q21.3) translocation with a breakpoint near the 5' end of the HOXB gene cluster in a patient with developmental delay and skeletal malformations. Eur J Hum Genet 15:570–577.

Journal of Human Genetics (2011) 56, 110–124

www.nature.com/jhg

ORIGINAL ARTICLE

Clinical application of array-based comparative genomic hybridization by two-stage screening for 536 patients with mental retardation and multiple congenital anomalies

Shin Hayashi[1,2], Issei Imoto[1,3], Yoshinori Aizu[4], Nobuhiko Okamoto[5], Seiji Mizuno[6], Kenji Kurosawa[7], Nana Okamoto[1,8], Shozo Honda[1], Satoshi Araki[9], Shuki Mizutani[9], Hironao Numabe[10], Shinji Saitoh[11], Tomoki Kosho[12], Yoshimitsu Fukushima[12], Hiroshi Mitsubuchi[13], Fumio Endo[13], Yasutsugu Chinen[14], Rika Kosaki[15], Torayuki Okuyama[15], Hirotaka Ohki[16], Hiroshi Yoshihashi[17], Masae Ono[18], Fumio Takada[19], Hiroaki Ono[20], Mariko Yagi[21], Hiroshi Matsumoto[22], Yoshio Makita[23], Akira Hata[24] and Johji Inazawa[1,25]

Recent advances in the analysis of patients with congenital abnormalities using array-based comparative genome hybridization (aCGH) have uncovered two types of genomic copy-number variants (CNVs); pathogenic CNVs (pCNVs) relevant to congenital disorders and benign CNVs observed also in healthy populations, complicating the screening of disease-associated alterations by aCGH. To apply the aCGH technique to the diagnosis as well as investigation of multiple congenital anomalies and mental retardation (MCA/MR), we constructed a consortium with 23 medical institutes and hospitals in Japan, and recruited 536 patients with clinically uncharacterized MCA/MR, whose karyotypes were normal according to conventional cytogenetics, for two-stage screening using two types of bacterial artificial chromosome-based microarray. The first screening using a targeted array detected pCNV in 54 of 536 cases (10.1%), whereas the second screening of the 349 cases negative in the first screening using a genome-wide high-density array at intervals of approximately 0.7 Mb detected pCNVs in 48 cases (13.8%), including pCNVs relevant to recently established microdeletion or microduplication syndromes, CNVs containing pathogenic genes and recurrent CNVs containing the same region among different patients. The results show the efficient application of aCGH in the clinical setting.
Journal of Human Genetics (2011) **56,** 110–124; doi:10.1038/jhg.2010.129; published online 28 October 2010

Keywords: array-CGH; congenital anomaly; mental retardation; screening

INTRODUCTION

Mental retardation (MR) or developmental delay is estimated to affect 2–3% of the population.[1] However, in a significant proportion of cases, the etiology remains uncertain. Hunter[2] reviewed 411 clinical cases of MR and reported that a specific genetic/syndrome diagnosis was carried out in 19.9% of them. Patients with MR often have congenital anomalies, and more than three minor anomalies can be useful in the diagnosis of syndromic MR.[2,3] Although chromosomal aberrations are well-known causes of MR, their frequency determined by conventional karyotyping has been reported to range from 7.9 to 36% in patients with MR.[4–8] Although the diagnostic yield depends on the population of each study or clinical conditions, such studies

[1]Department of Molecular Cytogenetics, Medical Research Institute and School of Biomedical Science, Tokyo Medical and Dental University, Tokyo, Japan; [2]Hard Tissue Genome Research Center, Tokyo Medical and Dental University, Tokyo, Japan; [3]Department of Human Genetics and Public Health Graduate School of Medical Science, The University of Tokushima, Tokushima, Japan; [4]Division of Advanced Technology and Development, BML, Saitama, Japan; [5]Department of Medical Genetics, Osaka Medical Center and Research Institute for Maternal and Child Health, Osaka, Japan; [6]Department of Pediatrics, Central Hospital, Aichi Human Service Center, Kasugai, Japan; [7]Division of Medical Genetics, Kanagawa Children's Medical Center, Yokohama, Japan; [8]Department of Maxillofacial Orthognathics, Graduate School, Tokyo Medical and Dental University, Tokyo, Japan; [9]Department of Pediatrics and Developmental Biology, Tokyo Medical and Dental University Graduate School, Tokyo, Japan; [10]Department of Medical Genetics, Kyoto University Hospital, Kyoto, Japan; [11]Department of Pediatrics, Hokkaido University Graduate School of Medicine, Sapporo, Japan; [12]Department of Medical Genetics, Shinshu University School of Medicine, Matsumoto, Japan; [13]Department of Pediatrics, Kumamoto University Graduate School of Medical Science, Kumamoto, Japan; [14]Department of Pediatrics, University of the Ryukyu School of Medicine, Okinawa, Japan; [15]Department of Clinical Genetics and Molecular Medicine, National Center for Child Health and Development, Tokyo, Japan; [16]The Division of Cardiology, Tokyo Metropolitan Children's Medical Center, Tokyo, Japan; [17]The Division of Medical Genetics, Tokyo Metropolitan Children's Medical Center, Tokyo, Japan; [18]Department of Pediatrics, Tokyo Teishin Hospital, Tokyo, Japan; [19]Department of Medical Genetics, Kitasato University Graduate School of Medical Sciences, Sagamihara, Japan; [20]Department of Pediatrics, Hiroshima Prefectural Hospital, Hiroshima, Japan; [21]Department of Pediatrics, Kobe University Graduate School of Medicine, Kobe, Japan; [22]Department of Pediatrics, National Defense Medical College, Saitama, Japan; [23]Education Center, Asahikawa Medical College, Asahikawa, Japan; [24]Department of Public Health, Chiba University Graduate School of Medicine, Chiba, Japan and [25]Global Center of Excellence (GCOE) Program for 'International Research Center for Molecular Science in Tooth and Bone Diseases', Tokyo Medical and Dental University, Tokyo, Japan
Correspondence: Professor J Inazawa, Department of Molecular Cytogenetics, Medical Research Institute, Tokyo Medical and Dental University, 1-5-45 Yushima, Bunkyo-ku, Tokyo 113-8510, Japan.
E-mail: johinaz.cgen@mri.tmd.ac.jp
Received 20 August 2010; revised 25 September 2010; accepted 30 September 2010; published online 28 October 2010

suggest that at least three quarters of patients with MR are undiagnosed by clinical dysmorphic features and karyotyping.

In the past two decades, a number of rapidly developed cytogenetic and molecular approaches have been applied to the screening or diagnosis of various congenital disorders including MR, congenital anomalies, recurrent abortion and cancer pathogenesis. Among them, array-based comparative genome hybridization (aCGH) is used to detect copy-number changes rapidly in a genome-wide manner and with high resolution. The target and resolution of aCGH depend on the type and/or design of mounted probes, and many types of microarray have been used for the screening of patients with MR and other congenital disorders: bacterial artificial chromosome (BAC)-based arrays covering whole genomes,[9,10] BAC arrays covering chromosome X,[11,12] a BAC array covering all subtelomeric regions,[13] oligonucleotide arrays covering whole genomes,[14,15] an oligonucleotide array for clinical diagnosis[16] and a single nucleotide polymorphism array covering the whole genome.[17] Because genome-wide aCGH has led to an appreciation of widespread copy-number variants (CNVs) not only in affected patients but also in healthy populations,[18–20] clinical cytogenetists need to discriminate between CNVs likely to be pathogenic (pathogenic CNVs, pCNVs) and CNVs less likely to be relevant to a patient's clinical phenotypes (benign CNVs, bCNVs).[21] The detection of more CNVs along with higher-resolution microarrays needs more chances to assess detected CNVs, resulting in more confusion in a clinical setting.

We have applied aCGH to the diagnosis and investigation of patients with multiple congenital anomalies and MR (MCA/MR) of unknown etiology. We constructed a consortium with 23 medical institutes and hospitals in Japan, and recruited 536 clinically uncharacterized patients with a normal karyotype in conventional cytogenetic tests. Two-stage screening of copy-number changes was performed using two types of BAC-based microarray. The first screening was performed by a targeted array and the second screening was performed by an array covering the whole genome. In this study, we diagnosed well-known genomic disorders effectively in the first screening, assessed the pathogenicity of detected CNVs to investigate an etiology in the second screening and discussed the clinical significance of aCGH in the screening of congenital disorders.

MATERIALS AND METHODS

Subjects

We constructed a consortium of 23 medical institutes and hospitals in Japan, and recruited 536 Japanese patients with MCA/MR of unknown etiology from July 2005 to January 2010. All the patients were physically examined by an expert in medical genetics or a dysmorphologist. All showed a normal karyotype by conventional approximately 400–550 bands-level G-banding karyotyping. Genomic DNA and metaphase chromosomes were prepared from peripheral blood lymphocytes using standard methods. Genomic DNA from a lymphoblastoid cell line of one healthy man and one healthy woman were used as a normal control for male and female cases, respectively. All samples were obtained with prior written informed consent from the parents and approval by the local ethics committee and all the institutions involved in this project. For subjects in whom CNV was detected in the first or second screening, we tried to analyze their parents as many as possible using aCGH or fluorescence *in situ* hybridization (FISH).

Array-CGH analysis

Among our recently constructed in-house BAC-based arrays,[22] we used two arrays for this two-stage survey. In the first screening we applied a targeting array, 'MCG Genome Disorder Array' (GDA). Initially GDA version 2, which contains 550 BACs corresponding to subtelomeric regions of all chromosomes except 13p, 14p, 15p, 21p and 22p and causative regions of about 30 diseases already reported, was applied for 396 cases and then GDA version 3, which contains 660 BACs corresponding to those of GDA version 2 and pericentromeric regions of all chromosomes, was applied for 140 cases. This means that a CNV detected by GDA is certainly relevant to the patient's phenotypes. Subsequently in the second screening we applied 'MCG Whole Genome Array-4500' (WGA-4500) that covers all 24 human chromosomes with 4523 BACs at intervals of approximately 0.7 Mb to analyze subjects in whom no CNV was detected in the first screening. WGA-4500 contains no BACs spotted on GDA. If necessary, we also used 'MCG X-tiling array' (X-array) containing 1001 BAC/PACs throughout X chromosome other than pseudoautosomal regions.[12] The array-CGH analysis was performed as previously described.[12,23]

For several subjects we applied an oligonucleotide array (Agilent Human Genome CGH Microarray 244K; Agilent Technologies, Santa Clara, CA, USA) to confirm the boundaries of CNV identified by our in-house BAC arrays. DNA labeling, hybridization and washing of the array were performed according to the directions provided by the manufacturer. The hybridized arrays were scanned using an Agilent scanner (G2565BA), and the CGH Analytics program version 3.4.40 (Agilent Technologies) was used to analyze copy-number alterations after data extraction, filtering and normalization by Feature Extraction software (Agilent Technologies).

Fluorescence *in situ* hybridization

Fluorescence *in situ* hybridization was performed as described elsewhere[23] using BACs located around the region of interest as probes.

RESULTS

CNVs detected in the first screening

In the first screening, of 536 cases subjected to our GDA analysis, 54 (10.1%) were determined to have CNV (Figure 1; Tables 1 and 2).

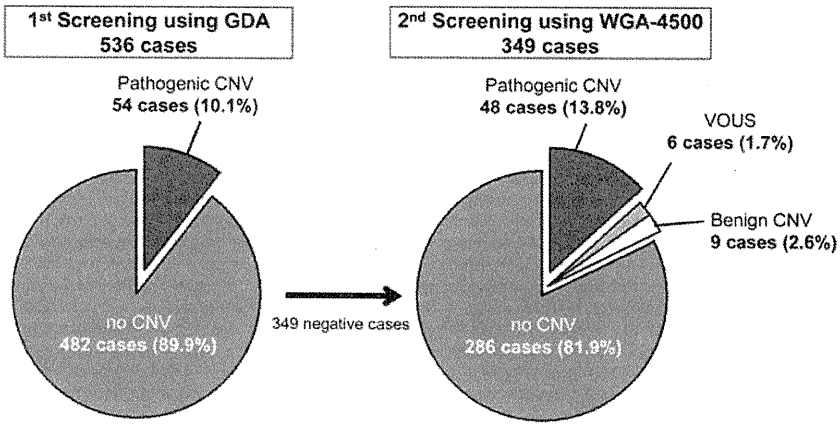

Figure 1 Percentages of each screening in the current study.

Table 1 A total of 40 cases with CNV at subtelomeric region(s) among 54 positive cases in the first screening

	Position where CNV detected				
Gender	*Loss*	*Gain*	*Corresponding disorder*[a]	*OMIM or citation*	*Parental analysis*[b]
M	1p36.33		Chromosome 1p36 deletion syndrome	#607872	
M	1p36.33p36.32		Chromosome 1p36 deletion syndrome	#607872	
M	1p36.33p36.32		Chromosome 1p36 deletion syndrome	#607872	
M	1p36.33p36.32		Chromosome 1p36 deletion syndrome	#607872	
M	1q44		Chromosome 1q43-q44 deletion syndrome	#612337	
F	2q37.3		2q37 monosomy[c]	Shrimpton *et al.*[24]	
F	2q37.3		2q37 monosomy[c]	Shrimpton *et al.*[24]	
M	3q29		Chromosome 3q29 deletion syndrome	#609425	
F	5p15.33p15.32		Cri-du-chat syndrome	#123450	
M	5q35.2q35.3		Chromosome 5q subtelomeric deletion syndrome	Rauch *et al.*[25]	
F	6p25.3		Chromosome 6pter-p24 deletion syndrome	#612582	
M	7q36.3		7q36 deletion syndrome[d]	Horn *et al.*[26]	
F	7q36.3		7q36 deletion syndrome[d]	Horn *et al.*[26]	
M	9p24.3p24.2		Chromosome 9p deletion syndrome	#158170	
F	9q34.3		Kleefstra syndrome	#610253	
F	10q26.3		Chromosome 10q26 deletion syndrome	#609625	
F	16p13.3		Chromosome 16p13.3 deletion syndrome	#610543	
F	22q13.31		Chromosome 22q13 deletion syndrome	#606232	
M	22q13.31q13.33		Chromosome 22q13 deletion syndrome	#606232	
M		15q26.3	15q overgrowth syndrome[c]	Tatton-Brown *et al.*[27]	
F		15q26.3	15q overgrowth syndrome[c]	Tatton-Brown *et al.*[27]	
M		21q22.13q22.3	Down's syndrome (partial trisomy 21)	#190685	
M		Xp22.33	A few cases have been reported; e.g. V5-130 in Lu *et al.*[28]		
M		Xq28	Chromosome Xq28 duplication syndrome	#300815	
F	1q44		Chromosome 1q43-q44 deletion syndrome	#612337	
		8p23.2p23.3			
M	3p26.3		3p deletion syndrome[d]	Fernandez *et al.*[29]	
		12p13.33p11.22			
F	3p26.3		3p deletion syndrome[d]	Fernandez *et al.*[29]	
		16p13.3	Chromosome 16p13.3 duplication syndrome	#613458	
F	4q35.2		4q– syndrome[d]	Jones *et al.*[30]	
		7q36.3			
M	5p15.33		Cri-du-chat syndrome	#123450	
		20p13			
M	5p15.33p15.32		Cri-du-chat syndrome	#123450	
		2p25.3			
F	6q27		6q terminal deletion syndrome[d]	Striano *et al.*[31]	
		11q25			
F	6q27		6q terminal deletion syndrome[d]	Striano *et al.*[31]	
		8q24.3			
M	7q36.3		7q36 deletion syndrome[d]	Horn *et al.*[26]	*dn*
		1q44			
M	9p24.3p24.2		Chromosome 9p deletion syndrome	#158170	
		7q36.3			
F	10p15.3p15.2		Chromosome 10p terminal deletion[d]	Lindstrand *et al.*[32]	*pat*
		7p22.3p22.2			
M	10p15.3		Chromosome 10p terminal deletion[d]	Lindstrand *et al.*[32]	
		2p25.3			
M	10q26.3		Chromosome 10q26 deletion syndrome	#609625	
		2q37.3	Distal trisomy 2q[d]	Elbracht *et al.*[33]	
M	18q23		Chromosome 18q deletion syndrome	#601808	
		7q36.3			
F	22q13.31q13.33		Chromosome 22q13.3 deletion syndrome	#606232	*pat*
		17q25.3	One case was reported	Lukusa *et al.*[34]	
M	Xp22.33/Yp11.32		Contiguous gene–deletion syndrome on Xp22.3[d]	Fukami *et al.*[35]	
		Xq27.3q28	Chromosome Xq28 duplication syndrome	#300815	

Abbreviations: F, female; CNV, copy-number variant; M, male; OMIM, Online Mendelian Inheritance in Man; *dn*, *de novo* CNV observed in neither of the parents.
[a]The name of disorder is based on entry names of OMIM, expect for entry names in DECIPHER and description in each cited article.
[b]*pat*, father had a balanced translocation involved in corresponding subtelomeric regions.
[c]Entry names in DECIPHER.
[d]Description in each cited article.

All the CNVs detected in the first screening were confirmed by FISH. Among the positive cases, in 24 cases one CNV was detected. All the CNVs corresponded to well-established syndromes or already described disorders (Table 1). In 16 cases two CNVs, one deletion and one duplication, were detected at two subtelomeric regions, indicating that one of parents might be a carrier with reciprocal translocation involved in corresponding subtelomeric regions, and at least either of the two CNVs corresponded to the disorders. We also performed parental analysis by FISH for three cases whose parental samples were available, and confirmed that in two cases the subtelomeric aberrations were inherited from paternal balanced translocation and in one case the subtelomeric aberrations were *de novo* (Table 1). In the other 14 cases, CNVs (25.9%) were detected in regions corresponding to known disorders (Table 2).

Table 2 Other cases among 54 positive cases in the first screening

	Position where CNV detected			
Gender	*Gain*	*Loss*	*Corresponding disorder*	*OMIM*
F		4p16.3	Ring chromosome	
		4q35.2		
M		3q22.323	BPES	#110100
M		2q22.3	ZFHX1B region	*605802
M		4q22.1	Synuclein (SNCA) region	*163890
F		7p21.1	Craniosynostosis, type 1	#123100
F		7q11.23	Williams syndrome	#194050
F		8q23.3q24.11	Langer–Giedion syndrome	#150230
M	15q11.2q13.1		Prader–Willi/Angelman	#176270/ #105830
F		17p11.2	Smith–Magenis syndrome	#182290
M		17q11.2	Neurofibromatosis, type I	+162200
M	22q11.21		DiGeorge syndrome	#188400
F		22q11.21	DiGeorge syndrome	#188400
F	Xp22.31		Kallmann syndrome 1	+308700
F	Whole X		Mosaicism	

Abbreviations: CNV, copy-number variant; F, female; M, male; OMIM, Online Mendelian Inheritance in Man.

CNVs detected in the second screening and assessment of the CNVs

Cases were subject to the second screening in the order of subjects detected no CNV in the first screening, and until now we have analyzed 349 of 482 negative cases in the first screening. In advance, we excluded highly frequent CNVs observed in healthy individuals and/or in multiple patients showing disparate phenotypes from the present results based on an internal database, which contained all results of aCGH analysis we have performed using WGA-4500, or other available online databases; for example, Database of Genomic Variant (http://projects.tcag.ca/variation/). As a result, we detected 66 CNVs in 63 cases (Figure 1; Table 3). Among them, three patients (cases 36, 42 and 44) showed two CNVs. All the CNVs detected in the second screening were confirmed by other cytogenetic methods including FISH and/or X-array. For 60 cases, we performed FISH for confirmation and to determine the size of each CNV. For five cases, cases 13, 36, 48, 57 and 63, with CNVs on the X chromosome, we used the X-array instead of FISH. For cases 4, 6, 16–19 and 34, we also used Agilent Human Genome CGH Microarray 244K to determine the refined sizes of CNVs. The maximum and minimum sizes of each CNV determined by these analyses are described in Table 3.

Well-documented pCNVs emerged in the second screening

CNVs identified for recently established syndromes. We assessed the pathogenicity of the detected CNVs in several aspects (Figure 2).[21,37,38] First, in nine cases, we identified well-documented pCNVs, which are responsible for syndromes recently established. A heterozygous deletion at 1q41–q42.11 in case 2 was identical to patients in the first report of 1q41q42 microdeletion syndrome.[39] Likewise a CNV in case 3 was identical to chromosome 1q43–q44 deletion syndrome (OMIM: #612337),[40] a CNV in case 4 was identical to 2q23.1 microdeletion syndrome,[41] a CNV in case 5 was identical to 14q12 microdeletion syndrome[42] and a CNV in case 6 was identical to chromosome 15q26-qter deletion syndrome (Drayer's syndrome) (OMIM: #612626).[43] Cases 7, 8 and 9 involved CNVs of different sizes at 16p12.1-p11.2, the region responsible for 16p11.2-p12.2 microdeletion syndrome.[44,45] Although an interstitial deletion at 1p36.23-p36.22 observed in case 1 partially overlapped with a causative region of chromosome 1p36 deletion syndrome (OMIM: #607872), the region deleted was identical to a proximal interstitial 1p36 deletion that was recently reported.[46] Because patients with the proximal 1p36 deletion including case 1 demonstrated different clinical characteristics from cases of typical chromosome 1p36 deletion syndrome, in the near term their clinical features should be redefined as an independent syndrome.[46]

CNVs containing pathogenic gene(s). In four cases we identified pCNVs that contained a gene(s) probably responsible for phenotypes. In case 10, the CNV had a deletion harboring *GLI3* (OMIM: *165240) accounting for Greig cephalopolysyndactyly syndrome (GCS; OMIM: 175700).[47] Although phenotypes of the patient, for example, pre-axial polydactyly of the hands and feet, were consistent with GCS, his severe and atypical features of GCS, for example, MR or microcephaly, might be affected by other contiguous genes contained in the deletion.[48] Heterozygous deletions of *BMP4* (OMIM: *112262) in case 11 and *CASK* (OMIM: *300172) in case 13 have been reported previously.[49,50] In case 12, the CNV contained *YWHAE* (OMIM: *605066) whose haploinsufficiency would be involved in MR and mild CNS dysmorphology of the patient because a previous report demonstrated that haploinsufficiency of *ywhae* caused a defect of neuronal migration in mice[51] and a recent report also described a microdeletion of *YWHAE* in a patient with brain malformation.[52]

Recurrent CNVs in the same regions. We also considered recurrent CNVs in the same region as pathogenic; three pairs of patients had overlapping CNVs, which have never been reported previously. Case 16 had a 3.3-Mb heterozygous deletion at 10q24.31–q25.1 and case 17 had a 2.0-Mb deletion at 10q24.32–q25.1. The clinical and genetic information will be reported elsewhere. Likewise, cases 14 and 15 also had an overlapping CNV at 6q12–q14.1 and 6q14.1, and cases 18 and 19 had an overlapping CNV at 10p12.1–p11.23. Hereafter, more additional cases with the recurrent CNV would assist in defining new syndromes.

CNVs reported as pathogenic in previous studies. Five cases were applicable to these criteria. A deletion at 3p21.2 in case 20 overlapped with that in one case recently reported.[53] The following four cases had CNVs reported as pathogenic in recent studies: a CNV at 7p22.1 in case 21 overlapped with that of patient 6545 in a study by Friedman *et al.*,[14] a CNV at 14q11.2 in case 22 overlapped with those of patients 8326 and 5566 in Friedman *et al.*,[14] a CNV at 17q24.1–q24.2 in case 23 overlapped with that in patient 99 in Buysse *et al.*[54] and a CNV at 19p13.2 in case 24 overlapped with case P11 in Fan *et al.*[55]

Large or gene-rich CNVs, or CNVs containing morbid OMIM genes. In cases inapplicable to the above criteria, we assessed CNVs

Table 3 Sixty-three cases with CNV in the 2nd screening

Case	Gender	Clinical diagnosis	Remarkable clinical features	CNV	Position	WGA-4500[b]	FISH[b]	Base position and size of the identified CNV[a]						Parental analysis	Protein-coding genes[c]	CNV assessment[d]	Corresponding or candidate gene(s)
								Start (max)	Start (min)	End (min)	End (max)	Size (min)	Size (max)				
1	M	MCA/MR		del	1p36.23p36.22	arr cgh 1p36.23p36.22 (RP11-81J7→RP11-199O1)x1	ish del(1)(p36.23p36.22) (RP11-462M3+, RP11-106A3-, RP11-28P4+)dn	8 585 127	8 890 860	10 561 097	11 143 717	1 670 237	2 558 590	*dn*	32	P	
2	M	MCA/MR		del	1q41q42.11	arr cgh 1q41 (RP11-135J2→RP11-239E10)x1	ish del(1)(q41q42.11) (RP11-706L9+, RP11-224O19-, RP11-367O4-)dn	215 986 492	216 532 600	221 534 398	222 467 931	5 001 798	6 481 439	*dn*	35	P	
3	F	MCA/MR	Epilepsy	del	1q44	arr cgh 1q44 (RP11-156E8)x1	ish del(1)(q44) (RP11-56O19+, RP11-156E8-)	241 996 973	243 177 632	243 251 660	244 141 010	74 028	2 144 037		11	P	
4	F	MCA/MR		del	2q22	arr cgh 2q23.1 (RP11-72H23)x1	ish del(2)(q23.1) (RP11-375H16-)	147 651 472	147 688 255	149 855 826	149 879 891	2 167 571	2 228 419		7	P	
5	F	MCA/MR		del	14q12q13.2	arr cgh 14q12q13.2 (RP11-369O9→RP11-26M6)x1	ish del(14)(q13.2) (RP11-831F6-)	28 768 137	29 297 829	34 689 412	35 489 337	5 391 583	6 721 200		25	P	
6	M	MCA/MR	CHD	del	15q26.2	arr cgh 15q26.2q26.3 (RP11-79C10→RP11-80F4)x1	ish del(15)(q26.2) (RP11-308P12-)	93 199 415	93 214 053	96 928 421	96 942 334	3 714 368	3 742 919		6	P	
7	M	MCA/MR	CHD	del	16p12.1p11.2	arr cgh 16p12.1p11.2 (RP11-309I14→RP11-150K5)x1	ish del(16)(p11.2) (RP11-75J11-)dn	25 795 340	27 008 538	29 825 404	31 443 492	2 816 866	5 648 152	*dn*	138	P	
8	M	MCA/MR	CHD	del	16p11.2	arr cgh 16p12.1p11.2 (RP11-360L15→RP11-150K5)x1	ish del(16)(p11.2) (RP11-360L15-, RP11-388M20+, RP11-75J11+)dn	27 184 508	28 873 631	29 825 404	31 443 492	951 773	4 258 984	*dn*	134	P	
9	F	MCA/MR		del	16p11.2	arr cgh 16p11.2 (RP11-368N21→RP11-499D5)x1	ish del(16)(p11.2) (RP11-388M20-, RP11-75J11-)	28 873 841	29 408 698	32 773 200	34 476 095	3 364 502	5 602 254		125	P	
10	M	MCA/MR		del	7p14.2p13	arr cgh 7p14.2p13 (RP11-138E20→RP11-52M17)x1	ish del(7)(p14.1p13) (RP11-258I11+, RP11-2J17-, RP11-346F12-)dn	35 621 006	36 470 190	44 657 334	45 508 196	8 187 144	9 887 190	*dn*	70	P	*GLI3*
11	F	MCA/MR	Corneal opacity	del	14q22.1q22.3	arr cgh 14q22.1q22.3 (RP11-122A4→RP11-172G1)x1	ish del(14)(q22.1) (RP11-122A4-, RP11-316L15+)dn	51 964 774	51 983 834	54 730 496	55 054 754	2 746 662	3 089 980	*dn*	18	P	*BMP4*
12	M	MCA/MR	Idiopathic leukodystrophy	del	17q13.3	arr cgh 17p13.3 (RP11-294J5→RP11-357O7)x1	ish del(17)(p13.3) (RP11-4F24-, RP11-26N6+)dn	1 008 128	1 146 211	2 077 151	2 026 967	930 940	1 018 839	*dn*	22	P	*YWHAE*
13	M	MCA/MR		del	Xp11.4p11.3	arr cgh Xp11.3p11.4 (RP11-1069J5→RP11-245M24)x1	ish del(X)(p11.4p11.3) (RP11-95C16-, RP11-829C10-)dn	41 392 291	41 385 453	45 419 624	45 495 709	4 034 171	4 103 418	*dn*	9	P	*CASK*

Table 3 Continued

Case	Gender	Clinical diagnosis	Remarkable clinical features	CNV	Position	WGA-4500[b]	FISH[b]	Base position and size of the identified CNV[a]						Parental analysis	Protein-coding genes[c]	CNV assessment[d]	Corresponding or candidate gene(s)
								Start (max)	Start (min)	End (min)	End (max)	Size (min)	Size (max)				
14	M	MCA/MR		del	6q12q14.1	arr cgh 6q12q14.2(RP11-502L6→RP11-232L4)x1	ish del(6)(q13)(RP11-28P18-)dn	69 029 871	69 731 888	83 926 178	85 101 718	14 194 290	16 071 847	*dn*	56	P	
15	M	ZLS		del	6q14.1	arr cgh 6q14.1(RP11-343P23→RP11-217L13)x1	ish del(6)(q14.1)(RP11-5N7-,RP11-990K4-,RP11-1I6+)	75 484 004	76 145 436	79 474 428	79 851 528	3 328 992	4 367 524		10	P	
16	F	MCA/MR	CHD	del	10p12.1p11.23	arr cgh 10p12.1p11.23(RP11-89D1→91A23)x1	ish del(10)(p12.1p11.23)(RP11-164A7-,RP11-110B21-)	27 045 285	27 054 002	29 057 401	29 088 950	2 003 399	2 043 665		18	P	
17	M	MCA/MR		del	10p12.1p11.23	arr cgh 10p12.1p11.23(RP11-218D6→RP11-RP11-181I11)x1	ish del(10)(p11.23)(RP11-15H10-)	28 121 596	28 131 608	30 559 024	30 577 807	2 427 416	2 456 211		12	P	
18	M	MCA/MR	CHD	del	10q24.31q25.1	arr cgh 10q24.31q25.1(RP11-108L7→RP11-108L7)x1	ish del(10)(q24.33)(RP11-416N2-)dn	102 560 783	102 568 462	105 914 057	105 929 608	3 345 595	3 368 825	*dn*	66	P	
19	M	MCA/MR		del	10q24.32q25.1	arr cgh 10q24.32q25.1(RP11-21N23→RP11-99N20)x1	ish del(10)(q24.33)(RP11-416N2-)dn	103 917 900	103 928 189	106 005 827	106 011 522	2 077 638	2 093 622	*dn*	41	P	
20	F	MCA/MR		del	3p21.31p21.2	arr cgh 3p21.31p21.2(RP11-24F11→RP11-89F17)x1	ish del(3)(p21.31)(RP11-3B7-)	46 150 261	46 359 965	51 390 597	52 571 544	5 030 632	6 421 283		175	P	
21	M	MCA/MR		del	7p22.1	arr cgh 7p22.1(RP11-90J23→RP11-2K20)x1	ish del(7)(p22.1)(RP11-2K20-)dn	3 185 609	5 892 225	6 233 987	6 409 277	341 762	3 223 668	*dn*	28	P	
22	F	MCA/MR	Corneal opacity, CHD	dup	14q11.2	arr cgh 14q11.2(RP11-152G22→RP11-84D12)x3	ish dup(14)(q11.2)(RP11-152G22++)	20 070 731	20 306 624	20 534 929	21 264 945	228 305	1 194 214		>30	P	
23	M	MCA/MR		del	17q24.1q24.2	arr cgh 17q24.1q24.2(RP11-89L7→RP11-79K13)x1	ish del(17)(q24.1q24.2)(RP11-93E5-,RP11-89L7-,RP11-79K13-)	60 576 365	60 936 391	64 592 701	64 587 782	3 656 310	4 011 417		29	P	
24	M	SMS susp.		del	19p13.2	arr cgh 19p13.2(RP11-197O4→RP11-164D24)x1	ish del(19)(p13.2)(91021-)	9 248 377	10 248 853	11 968 772	12 553 279	1 719 919	3 304 902	*dn*		P	
25	M	MCA/MR	Epilepsy	dup	2q11.2q13	arr cgh 2q11.2q13(RP11-90G13→RP11-79K7)x3	ish dup(2)(q11.2)(RP11-542D13++)	88 273 220	91 696 986	109 869 691	112 714 666	18 172 705	24 441 446		>30	P	
26	M	MCA/MR	CHD	dup	4p16.1	arr cgh 4p16.1(RP11-17I9)x3	ish dup(4)(p16.1)(RP11-301J10++)	8 202 790	8 520 479	9 793 705	10 638 054	1 273 226	2 435 264		17	P	

Table 3 Continued

Case	Gender	Clinical diagnosis	Remarkable clinical features	CNV Position	WGA-4500[b]	FISH[b]	Base position and size of the identified CNV[a]						Parental analysis	Protein-coding genes[c]	CNV assessment[d]	Corresponding or candidate gene(s)
							Start (max)	Start (min)	End (min)	End (max)	Size (min)	Size (max)				
27	F	MCA/MR		del 7q22.1q22.2	arr cgh 7q22.1q22.2 (RP11-10D8→ RP11-72J24)x1	ish del(7)(q22.1q22.2) (RP11-124G15+,RP11-188E1-,RP11-95P19-)	97 314 215	98 261 079	105 604 920	106 451 506	7 343 841	9 137 291		135	P	
28	F	MCA/MR	Epilepsy	del 12q13.13	arr cgh 12q13.13 (RP11-74I8→ RP11-624J6)x1	ish del(12)(q13.13) (RP11-624J6-)	50 987 232	51 016 427	51 956 291	52 180 088	939 864	1 192 856		44	P	
29	M	MCA/MR		dup 16q22.3	arr cgh 16q22.3 (RP11-90L19→ RP11-89K4)x3	ish dup(16)(q22.3) (RP11-115E3++, RP11-90L19++)	70 355 260	70 848 592	72 328 913	73 785 124	1 480 321	3 429 864		25	P	
30	M	RTS susp.		dup 16q24.1	arr cgh 16q24.1 (RP11-140K16→ RP11-442O1)x3	ish dup(16)(q24.1) (RP11-770B4++, RP11-140K16++)	82 699 729	82 797 548	83 749 375	84 123 857	951 827	1 424 128		16	P	
31	M	MCA/MR	Epilepsy	del 2q24.2q24.3	arr cgh 2q24.2 (RP11-89L13→ RP11-79L13)x1	ish del(2)(q24.2) (RP11-638N12-)	160 407 234	161 072 815	162 883 584	166 923 475	1 810 769	6 516 241		28	P	*TBR1*
32	M	MCA/MR		del 3p26.2	arr cgh 3p26.2 (RP11-32F23)x1	ish del(3)(p26.2) (RP11-32F23-)	3 943 353	4 016 797	4 198 468	4 329 970	181 671	386 617		2	P	*SUMF1*
33	M	MCA/MR	IgA deficiency	del 7q21.11	arr cgh 7q21.11 (RP11-22M18)x1	ish del(7)(q21.11) (RP11-115M2+, RP11-353O4-, RP11-22M18-)	83 597 839	83 601 541	84 549 609	84 788 160	948 068	1 190 321		3	P	*SEMA3A*
34	M	MCA/MR		dup 14q32.2	arr cgh 14q32.2 (RP11-128L1)x3	ish dup(14)(q32.2) (RP11-177F8++)	99 330 486	99 337 358	99 841 558	99 845 472	504 200	514 986		7	P	*EML1, YY1*
35	M	MCA/MR	Epilepsy	dup 16p13.3	arr cgh 16p13.3 (RP11-349I11)x3	ish dup(16)(p13.3) (RP11-349I11++)	4 851 459	5 678 447	5 906 909	6 165 923	228 462	1 314 464		9	P	*A2BP1*
36	M	MCA/MR		dup Xp22.2p22.13	arr cgh Xp22.2p22.13 (RP11-2K15→ RP11-115I10)x3	not performed (X-tiling array)	16 874 735	16 952 121	17 596 600	17 638 351	644 479	763 616		2	P	
				dup Xp21.3	arr cgh Xp21.3 (RP11-438J7)x3	not performed (X-tiling array)	28 704 076	28 704 076	28 868 075	28 868 075	163 999	163 999		1	P	*IL1RAPL1*
37	F	MCA/MR		del 1p34.3	arr cgh 1p34.3 (RP11-89N10→ RP11-416A14)x1	ish del(1)(p34.2) (RP11-195A8+, RP11-166F21-)dn	37 830 131	38 338 265	39 466 349	39 583 645	1 128 084	1 753 514	*dn*	7	P	
38	M	MCA/MR	Hyper IgE	dup 1q25.2	arr cgh 1q25.2 (RP11-177A2→ RP11-152A16)x3	ish dup(1)(1q25.2) (RP11-177A2++, RP11-152A16++)	177 088 480	177 196 858	177 535 659	177 859 828	338 801	771 348	*dn*	9	P	
39	M	MCA/MR		del 2p24.1p23.3	arr cgh 2p24.1p23.3 (RP11-80H16→ RP11-88F6)x1	ish del(2)(p23.3) (RP11-88F6-, RP11-373D23+)dn	20 037 821	23 094 244	26 815 794	28 414 457	3 721 550	8 376 636	*dn*	86	P	
40	F	MCA/MR	CHD	del 3p26.1p25.3	arr cgh 3p26.1p25.3 (RP11-128A5→ RP11-402P11)x1	ish del(3)(p26.1p25.3) (RP11-936E1-, RP11-402P11-, RP11-1079H21+) dn	8 190 557	8 497 949	9 930 973	10 026 217	1 433 024	1 835 660	*dn*	18	P	

Table 3 Continued

Case	Gender	Clinical diagnosis	Remarkable clinical features	CNV	Position	WGA-4500[b]	FISH[b]	Base position and size of the identified CNV[a]						Parental analysis	Protein-coding genes[c]	CNV assessment[d]	Corresponding or candidate gene(s)
								Start (max)	Start (min)	End (min)	End (max)	Size (min)	Size (max)				
41	M	MCA/MR		del	3p22.1p21.31	arr cgh 3p22.1p21.31 (RP11-241P3→ RP11-88B8)x1	ish del(3)(p22.1) (RP11-61H16+, RP11-241P3-, RP11-78O10+)dn	41 365 663	42 284 365	48 177 538	49 198 542	5 893 173	7 832 879	*dn*	123	P	
42	M	MCA/MR	Corneal opacity	del	3p14.3p14.2	arr cgh 3p14.3p14.2 (RP11-80H18→ RP11-79J9)x1	ish del(3)(p14.2) (RP11-79J19-, RP11-230A22+)mat	57 370 434	58 149 199	58 742 633	58 887 574	593 434	1 517 140	*mat*	11	B	
				del	8q21.11q21.13	arr cgh 8q21.11q21.13 (RP11-225J6→ RP11-214E11)x1	ish del(8) (q21.11q21.13) (RP11-225J6-, RP11-48B3+)dn	75 722 961	75 821 163	81 110 557	81 493 446	5 289 394	5 770 485	*dn*	12	P	
43	M	MCA/MR		del	3q26.31q26.33	arr cgh 3q26.31-q26.33 (RP11-292L5→ RP11-355N16)x1	ish del(3)(q26.32) (RP11-300L9+, RP11-105L6-)dn	175 650 310	176 531 688	180 613 203	181 653 281	4 081 515	6 002 971	*dn*	12	P	
44	M	MCA/MR	CHD	del	13q13.2q13.3	arr cgh 13q13.2 (RP11-269G10→ 90F5)x1	ish del(13)(q13.2) (RP11-142E9+, RP11-381E21-, RP11-98D3+)dn	33 451 136	33 895 560	34 813 379	34 909 905	917 819	1 458 769	*dn*	1	P	
				del	22q11.21	arr cgh 22q11.21 (RP11-155F20→ 54C2)x1	ish del(22)(q11.21) (RP11-155F20-, RP11-590C5-, RP11-54C2-)pat	19 310 307	19 310 307	19 590 642	19 590 642	280 335	280 335	*pat*	15	B	
45	F	aRS		del	18q21.2	arr cgh 18q21.2 (RP11-89B14)x1	ish del(18)(q21.2) (RP11-159D14+, RP11-186B13-, RP11-111C17-)dn	48 218 621	49 166 752	51 288 665	51 861 143	2 121 913	3 642 522	*dn*	9	P	
46	M	MCA/MR		dup	19p13.3	arr cgh 19p13.3 (RP11-49M3→ RP11-268O21)x3		1 095 485	2 418 857	3 499 581	4 460 252	1 080 724	3 364 767	*dn*	113	P	
47	F	MCA/MR	Autism	del	19p13.3	arr cgh 19p13.3 (RP11-30F17→ RP11-330I7)x1	ish del(19)(p13.3) (RP11-330I7-)dn	4 844 383	6 043 505	6 859 584	6 881 792	816 079	2 037 409	*dn*	23	P	
48	M	MCA/MR		del	Xp11.3	arr cgh Xp11.3 (RP11-151G3→ RP11-48J14)x0	ish del(X)(p11.3) (RP11-203D16-)mat	44 403 077	44 433 162	46 795 584	46 795 588	2 362 422	2 392 511	*mat*	18	P	
49	M	MCA/MR		dup	3p26.3	arr cgh 3p26.3 (RP11-630I)x3	ish dup(3)(p26.3) (RP11-630I++)pat	2 377 366	2 443 357	2 619 407	2 628 216	176 050	250 850	*pat*	1	B	
50	M	MCA/MR		dup	5p14.3	arr cgh 5p14.3 (RP11-91A5)x3	ish dup(5)(p14.3) (RP11-91A5++)pat	19 046 234	19 485 530	19 656 108	20 798 445	170 578	1 752 211	*pat*	1	B	
51	M	MCA/MR		dup	5q13.3	arr cgh 5q13.1 (RP11-40N8→ RP11-91C10)x3	ish dup(5)(q13.1) (RP11-105A11++)mat	66 417 271	66 481 371	67 501 700	67 838 977	1 020 329	1 421 706	*mat*	3	B	

Table 3 Continued

Case	Gender	Clinical diagnosis	Remarkable clinical features	CNV Position	WGA-4500[b]	FISH[b]	Base position and size of the identified CNV[a]						Parental analysis	Protein-coding genes[c]	CNV assessment[d]	Corresponding or candidate gene(s)
							Start (max)	Start (min)	End (min)	End (max)	Size (min)	Size (max)				
52	M	MCA/MR		dup 7p22.3	arr cgh 7p22.3 (RP11-23D23)x3	ish dup(7)(p22.3) (RP11-23D23++, RP11-1133D5+)mat	1	954 016	954 584	1 101 944	568	1 101 943	*mat*	12	B	
53	F	MCA/MR		dup 8p23.2	arr cgh 8p23.2 (RP11-79I19→ RP11-89I12)x3	ish dup(8)(p23.2) (RP11-89I19++, RP11-89I12++)pat	3 324 954	3 726 061	4 564 671	5 973 493	838 610	2 648 539	*pat*	1	B	
54	M	MCA/MR		dup 9q33.1	arr cgh 9q33.1 (RP11-150L1)x3	ish dup(9)(q33.1) (RP11-150L1++)pat	118 980 752	119 452 372	119 614 984	120 011 559	162 612	1 030 807	*pat*	2	B	
55	F	MCA/MR		dup 10q22.3	arr cgh 10q22.3 (RP11-79M9)x3	ish dup(10)(q22.3) (RP11-79M9++)mat	77 356 915	77 718 484	77 873 148	78 230 039	154 664	873 124	*mat*	1	B	
56	M	MCA/MR	ELBW, hepato-blastoma	dup 12q21.31	arr cgh 12q21.31 (RP11-91C4)x3	ish dup(12)(q21.31) (RP11-91C4++, RP11-142L2+)pat	80 924 954	82 678 148	82 830 190	85 768 388	152 042	4 843 434	*pat*	3	B	
57	M	GS		del Xp11.23	arr cgh Xp11.23 (RP11-876B24) x0 mat	not performed (X-tiling array)	47 752 808	47 747 918	47 852 109	47 868 412	104 191	115 604	*mat*	3	B	
58	M	MCA/MR		dup 8q11.23	arr cgh 8q11.23 (RP11-221P7)x3	ish dup(8)(q11.23) (RP11-221P7++, RP11-26P22++)	53 665 974	53 717 675	54 235 229	54 576 654	517 554	910 680		3	VOUS	
59	F	MCA/MR	Micro-cephaly	dup 10q11.21	arr cgh 10q11.21 (RP11-178A10)x3	ish dup(10)(q11.21) (RP11-178A10++)	41 986 946	42 197 693	42 320 775	43 603 027	123 082	1 616 081		15	VOUS	
60	M	MCA/MR		dup 11p14.2p14.1	arr cgh 11p14.2p14.1 (RP11-1L12)x3	ish dup(11) (p14.2p14.1) (RP11-1L12++)	26 723 462	27 033 270	27 213 374	27 445 504	180 104	722 042		4	VOUS	
61	F	MCA/MR		dup 12p11.1	arr cgh 12p11.1 (RP11-88P4)x3	ish dup(12)(p11.1) (RP11-472A10++)	33 333 493	33 359 944	33 572 956	33 572 956	213 012	239 463		2	VOUS	
62	F	aRS		dup 12q21.31	arr cgh 12q21.31 (RP11-91I24→ RP11-91C4)x3	ish dup(12)(q21.31) (RP11-91C4++, RP11-142L2++)	79 949 648	82 172 368	83 968 319	85 768 388	1 795 951	5 818 740		12	VOUS	
63	F	MR	Congenital myopathy	dup Xq12	arr cgh Xq12 (RP11-90P17→ RP11-383C12)x3	Not performed (X-tiling array)	66 212 661	66 216 353	66 921 699	66 948 538	705 346	735 877		1	VOUS	

Abbreviations: aRS, atypical Rett syndrome; B, benign; CNV, copy-number variant; *dn*: *de novo* CNV observed in neither of the parents; ELBW, extremely low birth weight; FISH, fluorescence *in situ* hybridization; GS, Gillespie syndrome; *mat*: CNV identified also in mother; P, pathogenic; *pat*: CNV identified also in father; RTS, Rubinstein–Taybi syndrome; SMS, Smith–Magenis syndrome; VOUS, variant of uncertain clinical significance; ZLS, Zimmermann–Laband syndrome.
[a]The sizes were estimated by WGA-4500, X-array, FISH or Agilent Human Genome CGH microarray 244K.
[b]The notation systems is based on ISCN2005.[36]
[c]The number of protein-coding genes contained in the respective CNVs.
[d]The result of CNV assessment.

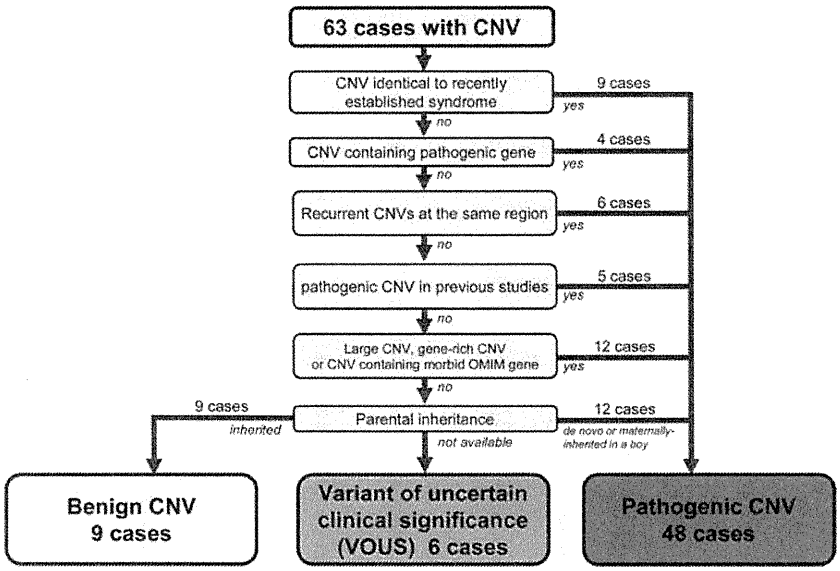

Figure 2 A flowchart of the assessment of CNVs detected in the second screening.

from several aspects. A CNV that contains abundant genes or is large (>3 Mb) has a high possibility to be pathogenic.[21] The CNVs in cases 25–30 probably correspond to such CNVs. Also, we judged a CNV containing a morbid OMIM gene as pathogenic:[21] *TBR1* (OMIM: *604616) in case 31,[56] *SUMF1* (OMIM: *607939) in case 32,[57,58] *SEMA3A* (OMIM: *603961) in case 33,[59] *EML1* (OMIM: *602033) and/or *YY1* (OMIM: *600013) in case 34,[60,61] *A2BP1* (OMIM: *605104) in case 35[62] and *IL1RAPL1* (OMIM: *300206) in case 36.[63] Several previous reports suggest that these genes are likely to be pathogenic, although at present no evidence of a direct association between these genes and phenotypes exists.

CNVs de novo or X maternally inherited. Among the remaining 27 cases, 12 cases had CNVs considered pathogenic as their CNVs were *de novo* (cases 37–47) or inherited del(X)(p11.3) from the mother (case 48). In the second screening we performed FISH for 36 CNVs of the 34 cases whose parental samples were available to confirm that 24 cases had *de novo* CNVs, which were probably pathogenic. A CNV in case 48, a boy with a nullizygous deletion at Xp11.3 inherited from his mother, was also probably relevant to his phenotype (Tables 3 and 4). Meanwhile, although case 57 was a boy with a deletion at Xp11.23 inherited from his mother, he was clinically diagnosed with Gillespie syndrome (OMIM: #206700) that was reported to show an autosomal dominant or recessive pattern,[64] thus we judged that the deletion was not relevant to his phenotype. As a result, cases 49–57 had only CNVs inherited from one of their parents which are likely to be unrelated to the phenotypes; that is, bCNV (Table 4).

As a result, we estimated that 48 cases among 349 analyzed (13.8%) had pCNV(s) in the second screening (Table 3; Figure 2). The CNVs of the remaining six cases, cases 58–63, were not associated with previously reported pathogenicity and their inheritance could not be evaluated, thus we estimated they were variants of uncertain clinical significance (VOUS).[38]

DISCUSSION

Because aCGH is a high-throughput technique to detect CNVs rapidly and comprehensively, this technique has been commonly used for analyses of patients with MCA and/or MR.[38,65–68] However, recent studies of human genomic variation have uncovered surprising properties of CNV, which covers 3.5–12% of the human genome even in healthy populations.[18–20,69] Thus analyses of patients with uncertain clinical phenotypes need to assess whether the CNV is pathogenic or unrelated to phenotypes.[21] However, such an assessment may diminish the rapidness or convenience of aCGH.

In this study, we evaluated whether our in-house GDA can work well as a diagnostic tool to detect CNVs responsible for well-established syndromes or those involved in subtelomeric aberrations in a clinical setting, and then explored candidate pCNVs in cases without any CNV in the first GDA screening. We recruited 536 cases that had been undiagnosed clinically and studied them in a two-stage screening using aCGH. In the first screening we detected CNVs in 54 cases (10.1%). Among them, 40 cases had CNV(s) at subtelomeric region(s) corresponding to the well-established syndromes or the already described disorders and the other 14 cases had CNVs in the regions corresponding to known disorders. Thus about three quarters of cases had genomic aberrations involved in subtelomeric regions. All the subtelomeric deletions and a part of the subtelomeric duplications corresponded to the disorders, indicating that especially subtelomeric deletions had more clinical significance compared to subtelomeric duplications, although the duplication might result in milder phenotypes and/or function as a modifier of phenotypes.[70] Moreover, parental analysis in three cases with two subtelomeric aberrations revealed that two of them were derived from the parental balanced translocations, indicating that such subtelomeric aberrations were potentially recurrent and parental analyses were worth performing. Recently several similar studies analyzed patients with MCA/MR or developmental delay using a targeted array for subtelomeric regions and/or known genomic disorders and detected clinically relevant CNVs in 4.4–17.1% of the patients.[28,65,70,71] Our detection rate in the first screening was equivalent to these reports. Although such detection rates depend on the type of microarray, patient selection criteria and/or number of subjects, these results suggest that at least 10% of cases with undiagnosed MCA/MR and a normal karyotype would be detectable by targeted array.

Table 4 Parental analysis of 34 cases in the second screening

Case	Gender	Clinical diagnosis	CNV del/dup	CNV Position	Size of CNV (bp) Min.	Size of CNV (bp) Max.	Protein-coding genes	Parental analysis	Pathogenicity
1	M	MCA/MR	del	1p36.23p36.22	1 670 237	2 558 590	32	*de novo*	P
2	M	MCA/MR	del	1q41q42.11	5 001 798	6 481 439	35	*de novo*	P
7	M	MCA/MR	del	16p12.1p11.2	2 816 866	5 648 152	138	*de novo*	P
8	M	MCA/MR with CHD	del	16p11.2	951 773	4 258 984	134	*de novo*	P
10	M	MCA/MR	del	7p14.2p13	8 516 513	9 421 233	70	*de novo*	P
11	F	MCA/MR	del	14q22.1q22.3	2 746 662	3 089 980	18	*de novo*	P
12	M	MCA/MR	del	17q13.3	930 940	1 018 839	22	*de novo*	P
13	M	MCA/MR	del	Xp11.4p11.3	4 034 171	4 103 418	9	*de novo*	P
14	M	MCA/MR	del	6q12q14.1	14 194 290	16 071 847	56	*de novo*	P
18	M	MCA/MR	del	10q24.31q25.1	3 345 595	3 368 825	66	*de novo*	P
19	M	MCA/MR	del	10q24.32q25.1	2 077 638	2 093 622	41	*de novo*	P
21	M	MCA/MR	del	7p22.1	341 762	3 223 668	28	*de novo*	P
24	M	SMS susp.	del	19p13.2	1 719 919	3 304 902	23	*de novo*	P
37	F	MCA/MR	del	1p34.3	1 128 084	1 753 514	7	*de novo*	P
38	M	MCA/MR	dup	1q25.2	338 801	771 348	9	*de novo*	P
39	M	MCA/MR	del	2p24.1p23.3	3 721 550	8 376 636	86	*de novo*	P
40	F	MCA/MR	del	3p26.1p25.3	1 433 024	1 835 660	18	*de novo*	P
41	M	MCA/MR	del	3p22.1p21.31	5 893 173	7 832 879	123	*de novo*	P
42[a]	M	MCA/MR	del	8q21.11q21.13	5 289 394	5 770 485	12	*de novo*	P
42[a]	M	MCA/MR	del	3p14.3p14.2	593 434	1 517 140	11	Maternal	B
43	M	MCA/MR	del	3q26.31q26.33	4 081 515	6 002 971	12	*de novo*	P
44[b]	M	MCA/MR	del	13q13.2q13.3	917 819	1 458 769	1	*de novo*	P
44[b]	M	MCA/MR	del	22q11.21	917 819	1 458 769	15	Paternal	B
45	F	Rett syndrome	del	18q21.2	2 121 913	3 642 522	9	*de novo*	P
46	M	MCA/MR	dup	19p13.3	2 041 395	2 404 096	113	*de novo*	P
47	F	MCA/MR	del	19p13.3	816 079	2 037 409	23	*de novo*	P
48[c]	M	MCA/MR	del	Xp11.3	2 362 422	2 392 511	18	Maternal	P
49	M	MCA/MR	dup	3p26.3	176 050	250 850	1	Paternal	B
50	M	MCA/MR	dup	5p14.3	170 578	1 752 211	1	Paternal	B
51	M	MCA/MR	dup	5q13.3	1 020 329	1 421 706	3	Maternal	B
52	M	MCA/MR	dup	7p22.3	568	1 101 943	12	Maternal	B
53	F	MCA/MR	dup	8p23.2	838 610	2 648 539	1	Paternal	B
54	M	MCA/MR	dup	9q33.1	162 612	1 030 807	2	Paternal	B
55	F	MCA/MR	dup	10q22.3	154 664	873 124	1	Maternal	B
56	M	MCA/MR	dup	12q21.31	152 042	4 843 434	3	Paternal	B
57	M	Gillespie syndrome	del	Xp11.23	104 191	115 604	3	Maternal	B

Abbreviations: B, benign; CNV, copy-number variant; F, female; M, male; MCA/MR, multiple congenital anomalies and mental retardation; P, pathogenic.
[a]Two CNVs were detected in case 42.
[b]Two CNVs were detected in case 44.
[c]Nullizygous deletion inherited from his mother probably affected the phenotype.

Another interesting observation in the first screening was that subtelomeric rearrangements frequently occurred even in patients with MCA/MR of uncertain whose karyotype had been diagnosed as normal. This result may be consistent with a property of subtelomeric regions whose rearrangements can be missed in conventional karyotyping,[72] and in fact other techniques involving subtelomeric FISH or MLPA also identified subtelomeric abnormalities in a number of patients with MCA and/or MR in previous reports.[70,73,74] Our result may support the availability of prompt screening of subtelomeric regions for cases with uncertain congenital disorders.

In the second screening we applied WGA-4500 to 349 cases to detect 66 candidate pCNVs in 63 cases (18.1%), and subsequently assessed the pathogenicity of these CNVs. The pCNVs included nine CNVs overlapping identical regions of recently recognized syndromes (cases 1–9; deletion at 1p36.23–p36.22, 1q41–q42.11, 1q43–q44, 2q23.1, 14q12, 15q26-qter and 16p11.2–p12.2, respectively), four CNVs containing disease-associated genes (cases 10–13; *GLI3*, *BMP4*, *YWHAE* and *CASK*, respectively), three pairs of CNVs of recurrent deletions (cases 14, 15: at 6q12–q14.1 and 6q14.1; case 16, 17: at 10p12.1–p11.23 and case 18, 19: at 10q24.31–q25.1 and 10q24.32–q25.1), five CNVs identical to pCNVs in previous studies (cases 20–24), six large and/or gene-rich CNVs (cases 25–30) and six CNVs containing a morbid OMIM gene (cases 31–36). For the remaining cases, we estimated the pathogenicity of the CNVs from a parental analysis (Table 4). We judged the 11 *de novo* CNVs (cases 37–47) and 1 CNV on chromosome Xp11.3 inherited from

the mother (case 48) as probably pathogenic. And nine inherited CNVs (cases 49–57) were probably benign. The clinical significance of CNVs in the other six cases, cases 58–63, remains uncertain (VOUS). As a result we estimated CNVs as pathogenic in 48 cases among 349 cases (13.8%) analyzed in the second screening. None of the pCNVs corresponded to loci of well-established syndromes. This may suggest that our two-stage screening achieved a good balance between rapid screening of known syndromes and investigation of CNV of uncertain pathogenicity.

Table 5 Summary of parental analyses

		Average size (bp)		*The average number of protein-coding genes*
		Min.	*Max.*	
Pathogenic CNVs[a]				
del	23	3 309 267	4 597 689	43
dup	2	1 190 098	1 587 722	61
Total	25	3 139 733	4 356 892	44
Benign CNVs[b]				
del	3	538 481	1 030 504	10
dup	8	334 432	1 740 327	3
Total	11	390 082	1 546 739	5

Abbreviation: CNV, copy-number variant.
[a]Twenty-four *de novo* CNVs and case 48.
[b]Eleven inherited CNVs other than case 48.

Among the cases with parental analyses, the 25 pCNVs had larger sizes and contained more protein-coding genes (average size, 3.1 Mb at minimum to 4.4 Mb at maximum; average number of genes, 44) as compared with the 11 inherited bCNVs that were probably unrelated to phenotypes (average size, 0.39 Mb at minimum to 1.5 Mb at maximum; average number of genes, 5) (Table 5). Although all of the 25 pCNVs except 2 were deletions, about three quarters (8 of 11 cases) of the inherited bCNVs were duplications (Table 5). These findings are consistent with previously reported features of pCNVs and bCNVs.[21,38]

We also compared our current study with recent aCGH studies meeting the following conditions: (1) a microarray targeted to whole genome was applied; (2) patients with MCA and/or MR of uncertain etiology, normal karyotype and the criteria for patients selection were clearly described; (3) pathogenicity of identified CNVs were assessed. On the basis of the above criteria, among studies reported in the past 5 years, we summarized 13 studies (Table 6).[10,14,15,17,54,55,75–81] Diagnostic yield of pCNVs in each study was 6.3–16.4%, and our current diagnostic yield of the second screening was 13.8%. Though cases with subtelomeric aberration detected in the first screening had been excluded, our diagnostic yield was comparable to those of the reported studies. It is not so important to make a simple comparison between diagnostic yields in different studies as they would depend on the conditions of each study, for example, sample size or array resolution,[38,82] however it seems interesting that the higher resolution of a microarray does not ensure an increase in the rate of detection of pCNVs. One recent study showed data that may explain the discrepancy between the resolution of microarray and diagnostic yield.[54,83] The authors analyzed 1001 patients with MCA and/or MR using one

Table 6 Previous studies of analyzing patients with MCA and/or MR using aCGH targeted to whole genome

	Applied array			*Patients*		*Pathogenic CNV*	
Author (year)	*Type*	*Number*[a]	*Distribution*[b]	*Number*	*Type of disorders*	*Number*	*%*
Schoumans *et al.*[75]	BAC	2600	1.0 Mb*	41	MCA and MR	4	9.8
de Vries *et al.*[76]	BAC	32 477	Tiling	100	MCA and/or MR	10	10.0
Rosenberg *et al.*[77]	BAC	3500	1.0 Mb*	81	MCA and MR	13	16.0
Krepischi-Santos *et al.*[78]	BAC	3500	1.0 Mb*	95	MCA and/or MR	15	15.8
Friedman *et al.*[14]	SNP	Affymetrix 100K	23.6 kb**	100	MR	11	11.0
Thuresson *et al.*[79]	BAC		1.0 Mb*	48	MCA and MR	3	6.3
Wagenstaller *et al.*[80]	SNP	Affymetrix 100K	23.6 kb**	67	MR	11	16.4
Fan *et al.*[55]	Oligo	Agilent 44K	24 kb–43 kb**	100[c]	MCA and MR, Autism	15[d]	15.0
Xiang *et al.*[15]	Oligo	Agilent 44K	24 kb–43 kb**	40[e]	MR, DD and autism	3	7.5
Pickering *et al.*[10]	BAC	2600	1 Mb*	354[f]	MCA and/or MR	36[g]	10.2
McMullan *et al.*[17]	SNP	Affymetrix 500K	2.5 kb–5.8 kb**	120	MCA and/or MR	18	15.0
Bruno *et al.*[81]	SNP	Affymetrix 250K	2.5 kb–5.8 kb**	117	MCA and/or MR	18	15.4
Buysse *et al.*[54]	BAC	3431	1 Mb*	298	MCA and/or MR	26	8.7
	Oligo	Agilent 44K	24 kb–43 kb**	703	MCA and/or MR	74	10.5
Our current study	BAC	4523	0.7 Mb	349	MCA and MR	48	13.8
Total				2613		305	11.7

Abbreviations: BAC, bacterial artificial chromosome; CNV, copy-number variant; DD, developmental delay; MCA, multiple congenital anomalies; MR, mental retardation; SNP, single nucleotide polymorphism.
[a]The number of clones or name of array is described.
[b]Each distribution referred to each article (*) or manual of each manufacturer (**).
[c]All cases were analyzed by both a targeted array and a genome-wide array.
[d]In five cases, CNVs were also identified by a targeted array.
[e]Ten cases with an abnormal karyotype were excluded.
[f]Only cases studied with an array throughout the genome are described. Ninety-eight cases were also analyzed by a targeted array.
[g]Seventeen cases with an abnormal karyotype were excluded.